

# MATERIALS CHEMISTRY

## FRONTIERS

## REVIEW



Cite this: *Mater. Chem. Front.*,  
2025, 9, 171

## Piezoelectric catalysis for antibacterial applications

Fanqing Meng,<sup>id</sup><sup>ab</sup> Chenxi Guo,<sup>a</sup> Tianchen Cui,<sup>b</sup> Mingyang Xu,<sup>a</sup> Xiaxia Chen,<sup>a</sup> Hongwei Xu,<sup>a</sup> Chao Liu<sup>a</sup> and Shaowei Chen<sup>id</sup><sup>\*,b</sup>

Efficient conversion of mechanical energy to electrical energy through piezoelectric catalysis has found diverse applications, such as sterilization, water treatment, organic synthesis, and biomass conversion. Among these, antibacterial agents based on piezoelectrically active materials have emerged as promising alternatives to conventional antibiotics for the treatment of bacterial diseases and remediation of water pollution caused by bacterial pathogens, with no bacterial resistance and side effects because of their fast and effective bactericidal actions. Herein, the general mechanisms of piezoelectric catalysis are reviewed, and commonly used piezoelectric antibacterial agents are highlighted, including semiconductors (metal oxides, metal sulfides, and ceramics), heterojunction composites (e.g., metal–semiconductor heterojunctions and semiconductor–semiconductor heterojunctions), and organic piezoelectric materials. Leading strategies for further enhancement of the materials' piezoelectric properties are also discussed, such as doping, compositing, and structural coupling. We conclude the review with a summary of the remaining challenges and a perspective for future research.

Received 26th September 2024,  
Accepted 4th December 2024

DOI: 10.1039/d4qm00848k

rsc.li/frontiers-materials

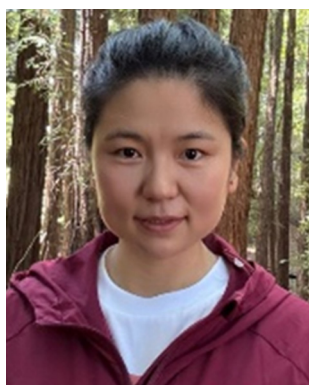
### 1. Introduction

Infectious diseases caused by pathogenic bacteria can have a serious impact on human health and cause huge losses to

economic activities, affecting social and economic development around the world.<sup>1,2</sup> According to statistics from the World Health Organization (WHO), pathogenic microorganisms transmitted by water cause more than three million deaths each year.<sup>3</sup> Antibiotics have played a pivotal role in combating bacterial infection;<sup>4</sup> however, the excessive use of antibiotics has led to the development of antibiotic resistance.<sup>5,6</sup> In fact, drug-resistant bacteria have caused about 700 000 deaths each year.<sup>7</sup> Traditional sterilization methods often require complex

<sup>a</sup>College of Chemical Engineering, Qingdao University of Science and Technology, Qingdao, Shandong 266042, China

<sup>b</sup>Department of Chemistry and Biochemistry, University of California, 1156 High Street, Santa Cruz, California 95064, USA. E-mail: shaowei@ucsc.edu



Fanqing Meng

*Fanqing Meng received her Master's and PhD degrees in Chemical Engineering and Technology from Dalian University of Technology in 2019. She then joined Qingdao University of Science and Technology as an Associate Professor. She is currently a visiting scholar in the Chen Lab at the University of California Santa Cruz. Her research interests focus on the design and engineering of nanocomposites as high-performance piezocatalysts for environmental remediation and water disinfection.*



Shaowei Chen

*Shaowei Chen finished his undergraduate study in 1991 with a BS degree in Chemistry from the University of Science and Technology of China (USTC), and then went to Cornell University receiving his MS and PhD degrees in 1993 and 1996, respectively. Following a postdoctoral appointment at the University of North Carolina at Chapel Hill, he started his independent career in Southern Illinois University in 1998. In the summer of 2004, he moved to UCSC and is currently a professor of chemistry. His research mainly focuses on nanoscale electron transfer and nanocomposite catalysts for energy conversion and storage.*

operation procedures, such as photocatalysis and ozone sterilization. Photocatalytic sterilization is based on the continuous illumination of a catalyst to induce electron–hole separation and hence reduction and oxidation reactions on the catalyst surface.<sup>8,9</sup> Ozone sterilization is generally executed with an ozone generator, which typically entails a small amount of ozone residues after operation that may impact the environment and human health.<sup>10–12</sup> Therefore, it is of both fundamental and technological significance to develop new antibacterial agents and sterilization technologies that are efficient, environmentally friendly, and feasible.

In recent years, piezoelectric catalysis (*i.e.*, piezocatalysis) has emerged as an attractive option. Piezocatalysis-based sterilization exploits the ubiquitous mechanical energy from the environment as a driving force to produce an electric field and trigger a series of chemical reactions, such as the production of reactive oxygen species (ROS) that can destroy bacterial cell walls, cell membranes, internal proteins, nucleic acids, and other organelles.<sup>13,14</sup> In contrast to traditional sterilization technologies, this operation requires no addition of chemical reagents, exhibits good selectivity, and is environmentally friendly and sustainable.<sup>15,16</sup> In addition, piezocatalysis can work efficiently at low energy consumption, and can precisely control the reaction process by manipulation of external stress parameters, leading to strong antibacterial controllability. This is critical in the development of new effective antibacterial agents to combat antibiotic resistance.<sup>17,18</sup>

In this review, we will start with a brief discussion of the mechanistic actions of piezocatalysis, followed by an overview of the antibacterial activity of a range of piezoelectric materials, such as metal oxides, metal sulfides, piezoelectric ceramics, metal–semiconductor heterojunctions, semiconductor–semiconductor heterojunctions, and organic piezoelectric catalysts. We conclude the review with a perspective highlighting the remaining challenges and future research directions for further development of the field.

## 2. Piezoelectric mechanisms

At present, although details of the piezoelectric mechanism have remained elusive, two primary theories are typically used to account for the piezoelectric properties, the energy band theory and the screening charge effect theory.<sup>13</sup> According to the energy band theory, the inherent electronic band structure, specifically, the conduction band (CB) and valence band (VB), plays a critical role in defining the catalytic activity for particular chemical reactions. In this context, the piezopotential serves as the driving force that alters the band levels, thereby enabling electrons and holes to gain the necessary energy to separate and participate in redox reactions. The screening charge effect emphasizes the significance of external screening charges in influencing the catalytic behaviors. In this theory, the piezopotential directly influences the material's reactivity, where the Gibbs free energy change ( $\Delta G$ ) must match or exceed that associated with the reaction. While both theories have successfully elucidated the piezoelectric effect in classic

reactions, such as those involved in water oxidation and dye degradation, they emphasize different aspects when it comes to controlling the reaction pathway and/or enhancing catalytic efficiency. The subsequent sections will delve into the theoretical basis of these two mechanisms and examine their distinct differences.

### 2.1. Energy band theory

The energy band theory is a theoretical framework in solid-state physics that describes and explains the electronic energy structure and conductivity of solid materials.<sup>19</sup> As shown in Fig. 1, a band consists of a range of energies that an electron is allowed to possess, where the filled band is called the VB and the unfilled band is called the CB. The energy difference between these two bands is the energy gap ( $E_g$ ), and the size of the energy gap determines the electrical conductivity of the material. The energy band theory is based on Bloch's theorem, which states that in a periodic potential field, the wave function of an electron can be expressed as the product of a plane wave and a periodic function. When the piezoelectric material is subjected to an external pressure or strain, its lattice structure may be slightly distorted or deformed. This shifts the electron wave function, resulting in the separation of positive and negative charges, forming a macroscopic electric dipole moment inside the crystal and hence the piezoelectric effect.<sup>20</sup>

### 2.2. Screening charge effect

The screening charge effect refers to the shielding or redistribution of charges in piezoelectric materials due to the rearrangement of electron clouds under the influence of an applied electric field.<sup>21</sup> As shown in Fig. 2, upon the application of an external electric field, the electron cloud inside the material can partially shield the external electric field, thereby weakening or enhancing the influence of the external electric field. This depends on the conductivity and dielectric constant of the material, and the mobility of the electrons, among others. Screening charge effects can help optimize the design

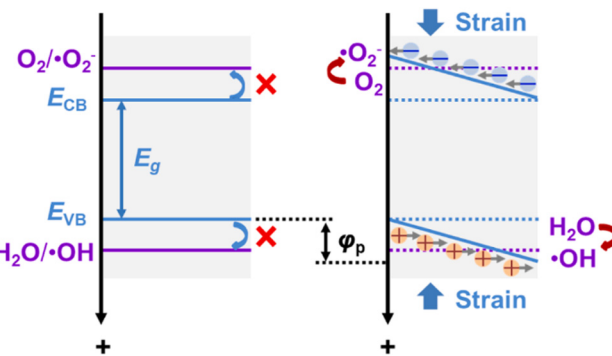


Fig. 1 Schematic illustration of the energy band theory for piezocatalysis, illustrated with the redox reactions of  $O_2 + e^- \rightarrow O_2^{\bullet-}$  and  $H_2O + h^+ \rightarrow OH^{\bullet}$ , where  $E_{CB}$  and  $E_{VB}$  are the positions of the CB and VB, respectively, and  $E_g$  and  $\varphi_p$  are the energy band gap and piezopotential, respectively. Reproduced with permission from ref. 19, copyright 2023, Elsevier.

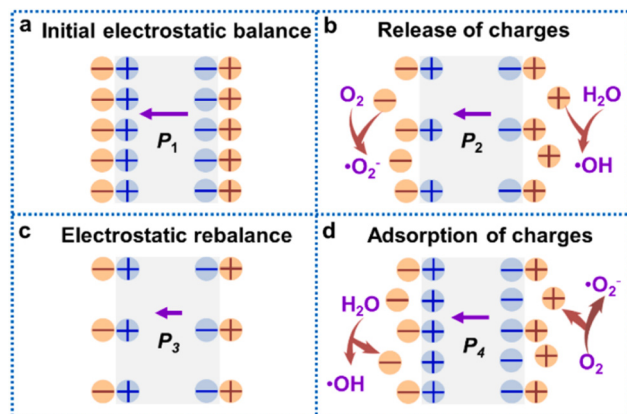


Fig. 2 Schematic description of the screening charge effect of piezocatalysis, where the orange and blue circles represent surface and bound charges, respectively, and  $P$  represents polarization: (a) the initial state of the electrostatic balance of an as-polarized piezoelectric material; (b) the release of screening charges to generate ROS when the material is subjected to a compressive strain; (c) the state of a new electrostatic balance after the minimization of bound charges; (d) the adsorption of charges from the electrolyte when the compressive strain is reduced. Reproduced with permission from ref. 19, copyright 2023, Elsevier.

of piezoelectric materials and customize materials with specific piezoelectric properties.<sup>22</sup> One can see that this theory is mostly relevant to materials with abundant internal charge carriers.

It should be noted that these two theories are not exclusive to each other. In practice, they may work collectively in dictating the piezoelectric properties and piezocatalytic performance.

### 2.3. Piezocatalysis-based antibacterial actions

Based on the above principles, piezocatalysis-based antibacterial therapy relies on mechanical stimulation to trigger a series of chemical and biological responses. When mechanical forces, such as vibration or ultrasound, are applied to piezoelectric materials at sites of bacterial infection, the deformation of the materials generates surface charges through the piezoelectric effect. These charges facilitate the production of reactive oxygen species (ROS) by interacting with adjacent oxygen or water molecules. As illustrated in Fig. 3, ROS, such as hydroxyl radicals ( $\cdot\text{OH}$ ), superoxide anions ( $\text{O}_2^{\cdot-}$ ), singlet oxygen ( $^1\text{O}_2$ ), and hydrogen peroxide ( $\text{H}_2\text{O}_2$ ), exert their antibacterial effects

by damaging bacterial cell membranes and/or causing oxidative stress *via* endocytosis. This leads to cellular dysfunction and eventual death. These reactive species are crucial for disrupting bacterial structural integrity and metabolic activity, which underpins the antibacterial mechanism.

## 3. Piezoelectric materials

The piezoelectric effect is produced only in crystals with no center of symmetry and caused by structural deformation of the crystal under the action of a mechanical force that leads to a relative displacement of the charge carriers and hence a change in the total electric moment of the crystal.<sup>23</sup> The piezoelectricity of a material is determined by its piezoelectric constants, the direct piezoelectric coefficient ( $d_{33}$ ,  $\text{pC N}^{-1}$ ) and the inverse piezoelectric coefficient ( $g_{33}$ ,  $\text{pm V}^{-1}$ ).<sup>24</sup> These two coefficients are measured in different ways, and cannot be directly converted, but they can be used to highlight and compare the difference in piezoelectric performance. Below is an overview of three leading representatives of piezoelectric materials.<sup>22</sup>

### 3.1. Piezoelectric ceramics

Piezoelectric ceramics represent a classical family of materials that can generate electric charges under mechanical stress. This unique property enables them to produce localized electric fields and ROS, which can effectively inactivate a wide range of microorganisms, including bacteria, viruses, and fungi. Common piezoelectric ceramics used for antimicrobial purposes include lead zirconate titanate (PZT), barium titanate ( $\text{BaTiO}_3$ ), and zinc oxide ( $\text{ZnO}$ ), each offering specific advantages in terms of piezoelectric coefficients, stability, and biocompatibility.<sup>25–28</sup> A schematic diagram of the piezocatalytic bacterial killing process is shown in Fig. 3. For instance, Shuai *et al.*<sup>27</sup> prepared polydopamine-coated  $\text{BaTiO}_3$  core-shell nanoparticles, achieving a maximum output current of 142 nA, a voltage of 10 V, and a bacterial inhibition rate exceeding 81%. Yao *et al.*<sup>29</sup> synthesized a series of potassium-sodium niobate piezoceramics with varying piezoelectric activity, ranging from 20 to 80  $\text{pC N}^{-1}$  under different polarization conditions. It was observed that these piezoceramics could effectively inhibit the growth of *Staphylococcus aureus* (*S. aureus*) bacterial colonies, promote the proliferation of rat bone marrow mesenchymal stem cells, and facilitate cell adhesion and spreading.

### 3.2. Transition metal sulfides

Transition metal sulfides represent another class of piezoelectric materials, such as molybdenum disulfide ( $\text{MoS}_2$ ), tungsten sulfide ( $\text{WS}_2$ ), copper disulfide ( $\text{Cu}_2\text{S}_3$ ), and so on.<sup>29–31</sup> For instance, Chen *et al.*<sup>32</sup> reported a piezoelectric coefficient ( $d_{33}$ ) of *ca.* 5.6  $\text{pC N}^{-1}$  for a  $\text{MoS}_2$  monolayer; and Zhou *et al.*<sup>33</sup> estimated the  $g_{33}$  coefficient of  $\text{WS}_2$  to be *ca.* 11.33  $\text{pm V}^{-1}$  from the amplitude response profiles in piezoresponse force microscopy (PFM) measurements. Although transition metal sulfides generally exhibit a lower piezoelectric coefficient (1–20  $\text{pC N}^{-1}$ ) than traditional piezoelectric ceramics (10–200  $\text{pC N}^{-1}$ ), they have attracted significant interest due to their unique catalytic properties.<sup>31</sup>

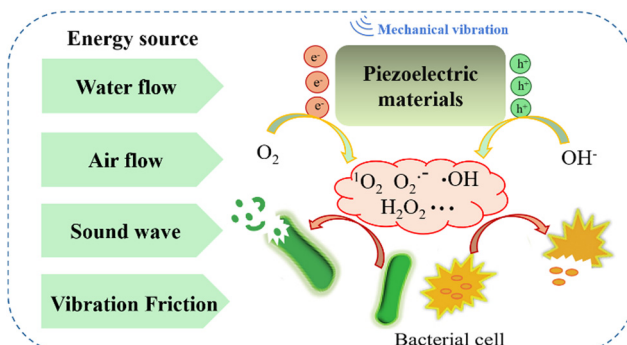


Fig. 3 Schematic diagram of the piezocatalytic bacterial killing process.

In fact, transition metal dichalcogenides offer notable advantages in flexibility and compatibility with two-dimensional materials, making them promising candidates for integration into flexible electronics and piezocatalytic devices. Current research efforts have been focused on enhancing their piezoelectric properties through strategies like doping, strain engineering, and formation of heterostructures (for examples, see Section 4), which can expand their applications into various technological fields.

### 3.3. Piezoelectric polymers

Select polymers also exhibit piezoelectric properties, such as polyvinylidene fluoride (PVDF), polyvinylidene fluoride-trifluoroethylene copolymer (PVDF-TrFE), poly-L-lactic acid (PLLA), polyimide, polyvinyl acetate (PVAc), poly(3-hexylthiophene) (P3HT), and silicone polymers, and have been exploited for antibacterial applications. These materials typically feature a piezoelectric coefficient of 5 to 100  $\text{pC N}^{-1}$ . Under mechanical stress, they are capable of generating electrical charges, which can effectively disrupt bacterial cell membranes, leading to bacterial cell destruction.<sup>29,31,34,35</sup> The electric fields generated by these materials can lead to the formation of ROS, which are known to cause oxidative stress and damage to bacterial cells, ultimately inhibiting their growth and survival.<sup>36</sup> As shown in Fig. 4, Singh *et al.* reported that PVDF-based piezoelectric materials could achieve up to 98% elimination of *S. aureus* and 95% elimination of *Escherichia coli* (*E. coli*) within 24 h of exposure.<sup>34</sup> These materials generated localized electric fields that facilitated the production of ROS causing oxidative stress and damage to bacterial cells, thereby eradicating the bacteria.<sup>29</sup> Moreover, the incorporation of silver nanoparticles into PVDF matrices has been shown to enhance the antibacterial efficacy, with up to 99% reduction in bacterial colonies.<sup>37</sup> This makes piezoelectric polymers promising

candidates for applications in medical devices, wound dressings, and surface coatings, where effective bacterial inhibition is critical to prevent infections.

Among these three types of piezoelectric materials, transition metal sulfides typically exhibit a relatively low piezoelectric coefficient (under 200  $\text{pC N}^{-1}$ ) but possess significant piezocatalytic activity, making them suitable for applications in energy harvesting and environmental remediation.<sup>33</sup> Yet, despite good thermal and chemical stability, the low mechanical strength limits their broad applications. In contrast, piezoelectric ceramics are characterized by the highest piezoelectric coefficients (200–1000  $\text{pC N}^{-1}$ ) and hence excellent efficiency in transducer applications.<sup>32</sup> Although the piezocatalytic activity is relatively low, these materials demonstrate exceptional stability under high temperatures and mechanical stress, thereby a prolonged service life. For piezoelectric polymers, they possess unique advantages such as flexible and lightweight structures, but a low piezoelectric coefficient (50–100  $\text{pC N}^{-1}$ ) and limited piezocatalytic activity.<sup>35</sup> Also, the thermal and mechanical stability is generally inferior to that of ceramics, which restricts their performance in harsh environments. Therefore, in practical sterilization applications, it is crucial to select materials based on specific requirements and to enhance the properties by the formation of composite materials through appropriate coupling strategies (for examples, see Section 4).

## 4. Piezocatalysis in antibacterial applications

Upon mechanical stress, piezoelectric materials can generate electric charges that react with water and/or dissolved oxygen molecules, producing ROS such as hydrogen peroxide and hydroxyl radicals.<sup>34,38</sup> These active species are highly effective in killing bacteria by damaging their cell membranes, DNA, and other vital cellular components. Unlike traditional antibacterial methods that often rely on chemical disinfectants, heat, or UV light, piezocatalysis can be activated by simple mechanical forces, such as vibrations or ultrasonic waves, enabling continuous and controllable antibacterial activity without the need for external light, heat, or chemical additives. This makes piezocatalytic materials suitable and attractive for a wide range of applications, *e.g.*, healthcare, food safety, and environmental sanitation.<sup>36</sup>

Additionally, piezocatalysis can operate under mild conditions, generate no harmful by-products, and offer a more sustainable and eco-friendlier alternative to conventional antibacterial strategies. Current research has been mostly focusing on optimizing the efficiency of piezocatalytic materials and understanding their underlying mechanisms to further enhance antibacterial performance.<sup>31</sup>

As shown in Fig. 5a and b, polarization of the piezocatalysts (such as  $\text{ZnO}$  and  $\text{BaTiO}_3$ ) can provide a remote driving force for the effective separation of electron–hole pairs, and their spatial transmission in opposite directions results in the displacement of the centers of the positive and negative charges

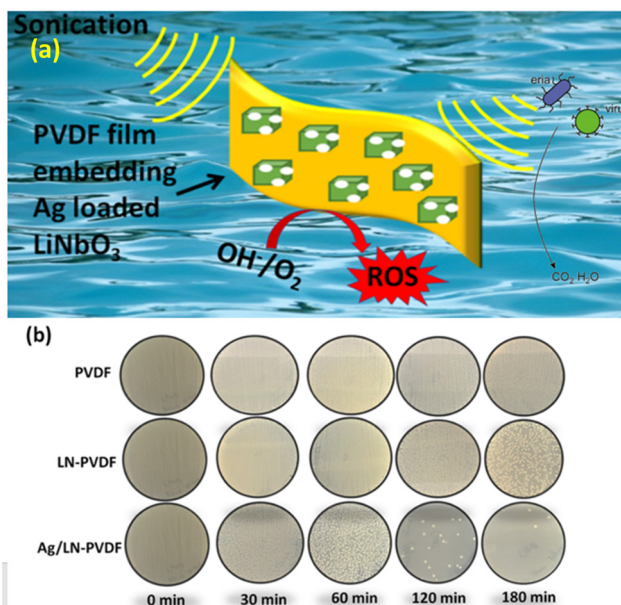


Fig. 4 Sterilization of PVDF-based piezoelectric catalysts. (a) Piezocatalytic mechanism and (b) sterilization results against *S. aureus*. Reproduced with permission from ref. 34, copyright 2021, the American Chemical Society.

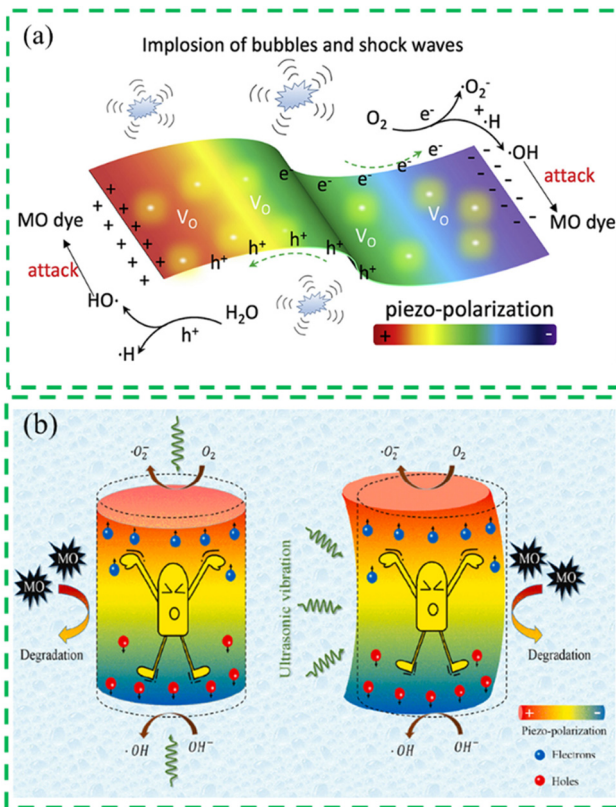
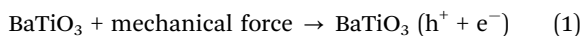


Fig. 5 Piezocatalytic degradation of dye pollutants. (a) Change in the electronic structure of ZnO/Al<sub>2</sub>O<sub>3</sub> composite in a piezocatalytic degradation reaction. Reproduced with permission from ref. 37, copyright 2020, Elsevier. (b) The role of the BaTiO<sub>3</sub> nanowire microstructure in piezocatalytic degradation of organic dye pollutants in wastewater. Reproduced with permission from ref. 39, copyright 2019, Elsevier.

and the formation of an internal electric field, leading to the accumulation of a large number of electrons and holes on the catalyst surface.<sup>37,39</sup>

These charges can then react with water and/or dissolved oxygen to form ROS, such as superoxide anions (O<sub>2</sub><sup>•-</sup>) and hydroxyl radicals (•OH), that facilitate the degradation of organic pollutants and water disinfection.<sup>40-43</sup> From Fig. 6a, one can see that the produced ROS can attack bacterial cell membranes, cell walls, and organelles,<sup>44</sup> leading to destruction of the cell structure and eventually cell death.<sup>45</sup> With BaTiO<sub>3</sub> as the illustrating example (Fig. 6b), the reactions can be summarized as follows:



The produced ROS reacts non-discriminately with a wide variety of components of the bacterial cells, leading to cell death (Fig. 6c and d).<sup>15,47</sup>

Recent studies have shown that the piezoelectric catalytic bactericidal performance can be improved by regulating the

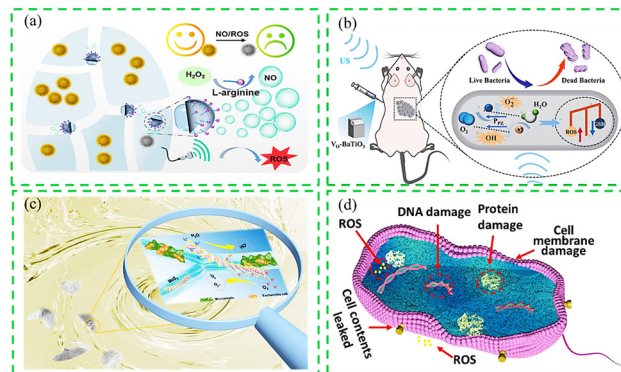


Fig. 6 Schematic illustration of the piezoelectric antibacterial mechanism. (a) and (c) The generation mechanism of ROS during the water flow process. (b) and (d) Reactions of piezo-generated ROS with bacterial cells. Panel (a) was reproduced with permission from ref. 15, copyright 2022, the American Chemical Society. Panel (b) was reproduced with permission from ref. 44, copyright 2024, the American Chemical Society. Panel (c) was reproduced with permission from ref. 45, copyright 2023, the American Chemical Society. Panel (d) was reproduced with permission from ref. 46, copyright 2021, the American Chemical Society.

morphology and band structure of the materials.<sup>43,44,48</sup> As shown in Fig. 7a-c, Lei *et al.*<sup>46</sup> synthesized an ultrasound-responsive sulfur-doped barium titanate (SDBTO) piezoelectric catalyst and observed a high  $g_{33}$  coefficient of 13.95 pm V<sup>-1</sup>. This catalyst demonstrated an exceptional piezocatalytic performance, with an antibacterial efficiency of 97.12% against *S. aureus*, mainly due to the highly active ROS produced under ultrasound (Fig. 7d). In another study, Liu *et al.*<sup>49</sup> designed a multifunctional ultrasound-triggered piezoelectric composite hydrogel (UPCH) with a  $d_{33}$  coefficient of 20.4 pC N<sup>-1</sup>. Under ultrasound stimulation, the UPCH produced a piezoelectric current of 0.38  $\mu$ A cm<sup>-2</sup> and a notable antibacterial performance, as manifested in the large fraction of bacteria with red fluorescence (dead bacteria) at 98.5% for *E. coli* and 97.4% for *S. aureus*. Ding *et al.*<sup>50</sup> reported a BaTiO<sub>3</sub> bionanocarrier that could generate a piezoelectric current of 0.2 mA under mechanical stress. Under the synergistic actions of near-infrared (NIR) and ultrasound irradiations, the BaTiO<sub>3</sub> nanocarrier produced a large amount of ROS, destroyed bacterial cell membranes, thereby achieving a bactericidal rate up to 99.8%.

#### 4.1. Transition metal oxides

Metal oxide piezoelectric materials are widely recognized for their effectiveness in antibacterial applications. These materials, including zinc oxide (ZnO) and titanium dioxide (TiO<sub>2</sub>), are known for their ability to generate ROS when subjected to external stimuli such as ultrasonic vibrations or light exposure.<sup>43,51-53</sup> As shown Fig. 8, the generated hydroxyl radicals and superoxide ions can damage bacterial cell membranes, leading to cell death. Improving the piezoelectric properties of these materials can facilitate the generation of ROS through mechanical stress or electric fields, thereby enhancing their antibacterial efficacy.<sup>51</sup>

For instance, Banerjee *et al.*<sup>51</sup> synthesized a ZnO/chitosan (ZnO/CHS) nanocomposite for bactericidal applications. Upon

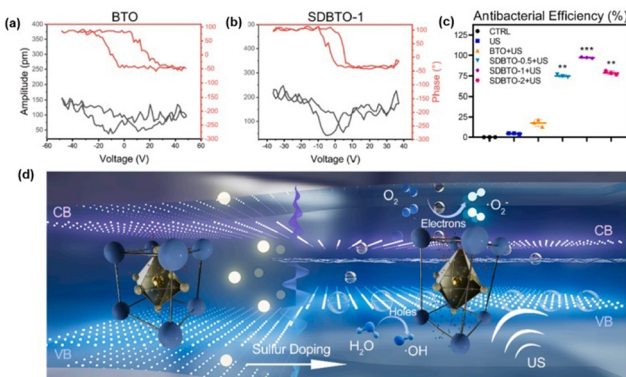


Fig. 7 Piezoelectric characterization and antibacterial mechanism. (a) and (b) Plots of PFM amplitude and hysteresis loop of BTO and SDBTO. (c) Quantified antibacterial efficiency of the as-prepared piezocatalysts. (d) Schematic illustration of the piezocatalytic antibacterial mechanism. Reproduced with permission from ref. 46, copyright 2022, Elsevier.

the application of ultrasonic irradiation for 20 min (Fig. 9a), ZnO/CHS achieved a removal rate of 96% against *Enterococcus faecalis* (*E. faecalis*) and 98% against *E. coli*. Scanning electron microscopy (SEM) measurements (Fig. 9b-d and f) show that the nanocomposite induced perforations and significant distortion of the bacterial cells under ultrasonic vibrations, leading to membrane rupture. In addition, from Fig. 9e, one can see that under ultrasonic irradiation, the ZnO/CHS composite facilitated the effective generation of ROS as manifested by the intense fluorescence emission of dichlorofluorescein (D), whereas the fluorescence intensity was markedly lower with ZnO/CHS (B) or ultrasonic (C) alone, and minimal with the blank (A). This indicates that the synergistic effect of nanocomposites and ultrasound played a key role in the high intracellular oxidant generation and hence bactericidal activity.

#### 4.2. Transition metal sulfides

Transition metal sulfides, *e.g.*, MoS<sub>2</sub> and WS<sub>2</sub>, have also emerged as promising antibacterial agents due to their unique piezoelectric properties, despite relatively low piezoelectric coefficients (5–20 pC N<sup>-1</sup>) as compared to traditional piezoelectric ceramics. For instance, Chen *et al.*<sup>32</sup> prepared a series

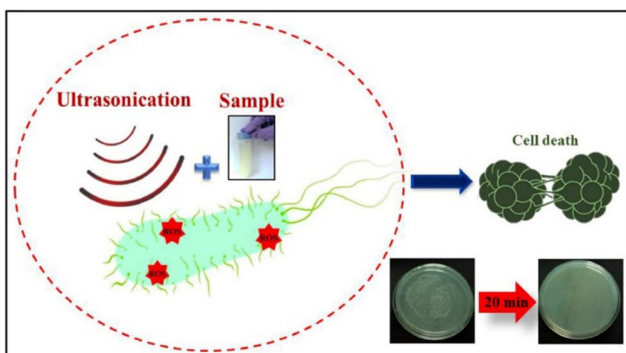


Fig. 8 Schematic illustration of the ROS mechanism and pathogenic bacterial degradation. Reproduced with permission from ref. 51, copyright 2024, Elsevier.

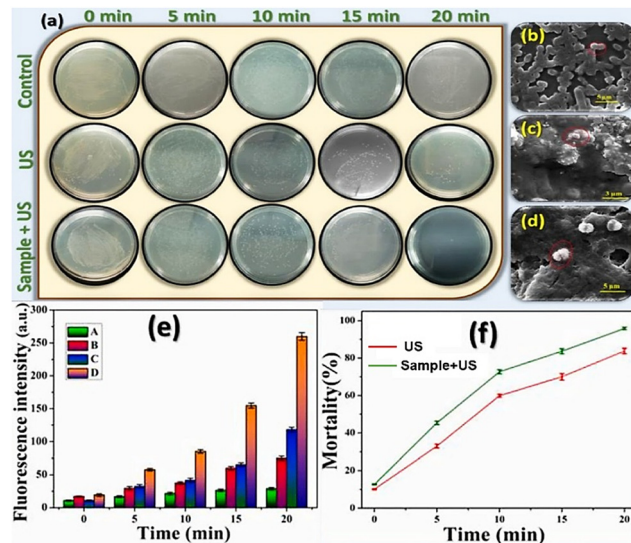
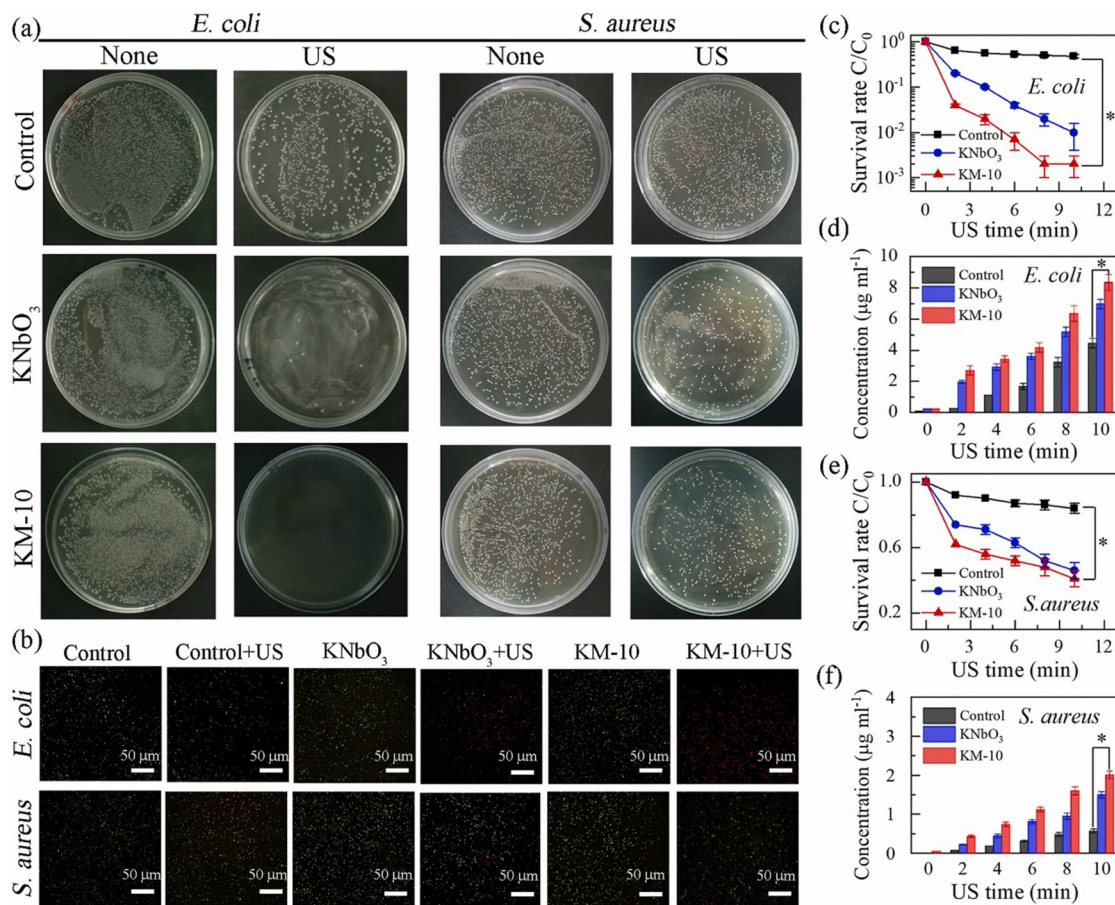


Fig. 9 Antibacterial activity of ZnO/CHS nanocomposite against *E. faecalis* and *E. coli*. (a) In comparison to the control, digital photos of the surviving colonies on agar plates after the incubation period under various circumstances. (b)–(d) FESEM micrographs of *E. faecalis* exhibiting higher membrane rupture into smaller size fractions as compared to the control. (e) Fluorescence intensity as a function of time: A (control), B (ZnO/CHS composite alone), C (ultrasound only), and D (ZnO/CHS composite and ultrasound), and (f) mortality percentage. Reproduced with permission from ref. 51, copyright 2023, Elsevier.

of sulfur-vacant and boron-doped MoS<sub>2</sub> (Vs-B/MoS<sub>2</sub>) piezoelectric materials ( $d_{33} = ca. 35.1 \text{ pC N}^{-1}$ ), which could produce ROS under mechanical stress and effectively inactivate bacteria. Luo *et al.*<sup>54</sup> prepared a KNbO<sub>3</sub>/MoS<sub>2</sub> heterojunction composed of KNbO<sub>3</sub> and MoS<sub>2</sub> nanosheets by a simple two-step hydrothermal method and observed a potential difference of 282.0 mV. Under mechanical stress, the heterojunctions generated a piezoelectric current of  $0.13 \text{ mA cm}^{-2}$ . The formation of heterojunctions and the polarized interfacial electrical field greatly enhanced the separation and transport of free electrons and holes and promoted the generation of O<sub>2</sub><sup>•</sup> and •OH radicals, resulting in highly efficient antibacterial activity. As shown in Fig. 10a, one can see that for the control group (*E. coli* and *S. aureus*) ultrasound treatment alone led to only a small decrease in the number of bacterial colonies, and there was a negligible difference in bacterial growth in the presence and absence of the heterojunction catalyst but without sonication. Yet upon the application of ultrasonic irradiation, the survival rate of *E. coli* was gradually decreased with increasing ultrasound time, and almost no bacterial colony could be found after 10 min of treatment, corresponding to an antibacterial rate as high as 99.77%. Notably, the antibacterial effect of the KNbO<sub>3</sub>/MoS<sub>2</sub>-10 sample (with 10 wt% MoS<sub>2</sub>) towards *E. coli* was greater than toward *S. aureus* (Fig. 10c and e), suggesting that *E. coli* was more susceptible to electrical stimulation than *S. aureus*, likely due to the abundant peptidoglycans in the cell walls of *S. aureus* that resulted in thicker and harder bacterial membranes.<sup>51,54</sup> It can be seen that the inhibitory rate of KNbO<sub>3</sub> against *E. coli* and *S. aureus* was lower than that of KNbO<sub>3</sub>/MoS<sub>2</sub>-10. The bacterial survival was also tested by



**Fig. 10** Piezocatalytic antibacterial effect of  $\text{KNbO}_3/\text{MoS}_2$  (KM-x) heterojunction composites against *E. coli* and *S. aureus*. (a) Photographs of colonies, (b) fluorescent images of live/dead staining of *E. coli* and *S. aureus* under various treatments, (c) and (e) survival rate and (d) and (f) protein leakage analysis of (c) and (d) *E. coli* and (e) and (f) *S. aureus*. Reproduced with permission from ref. 54, copyright 2023, Elsevier.

live/dead staining. As shown in Fig. 10b, all bacteria died in the  $\text{KNbO}_3/\text{MoS}_2$ -10 solution, while bacteria in the control group and ultrasound group survived, consistent with the bacterial survival rates. The amount of protein leakage from the bacteria increased with prolonged ultrasonic treatment; and  $\text{KNbO}_3/\text{MoS}_2$ -10 produced the largest protein leakage after 10 min of ultrasonic treatment at  $8.35 \mu\text{g mL}^{-1}$  for *E. coli* (Fig. 10d) and  $2.01 \mu\text{g mL}^{-1}$  for *S. aureus* (Fig. 10f). The outstanding antibacterial efficiency was attributed to the high surface area and high pore volume density of the  $\text{KNbO}_3/\text{MoS}_2$ -10 heterojunction, which killed bacteria through the force generated by the piezoelectric effect enhanced by the  $\text{KNbO}_3/\text{MoS}_2$  heterojunction that boosted the formation of free electrons and hole-generated ROS.

#### 4.3. Piezoelectric ceramics

Piezoelectric ceramics have been extensively utilized in antibacterial applications due to their high piezoelectric coefficients and robust mechanical properties. Notable examples include lead zirconate titanate (PZT),  $\text{KNbO}_3$  and barium titanate ( $\text{BaTiO}_3$ ), which convert mechanical energy into electrical energy, leading to the generation of ROS and/or electrical fields that can disrupt bacterial cells.<sup>55–63</sup> For example, Liao *et al.*<sup>63</sup> reported that the piezoelectric properties of potassium

sodium niobate (KNN) could be improved by regulating their microstructure, and the optimized (K, Na)-doped  $\text{NbO}_3$  exhibited a degradation rate over 90% against organic pollutants in aqueous media under ultrasound activation. Lei *et al.*<sup>46</sup> synthesized an ultrasound-responsive sulfur-doped barium titanate (SDBTO) piezocatalyst, which exhibited a superior antibacterial performance with a 97.12% inhibition efficiency against *S. aureus* after ultrasonic treatment for 45 min in the presence of  $1 \text{ mg mL}^{-1}$  nanoparticles. Wei *et al.*<sup>64</sup> synthesized  $\text{BaTiO}_3$  hollow nanoparticles doped with cerium ( $\text{hBT}_{\text{Ce}}$ ) to improve their piezocatalytic antibacterial properties, due to an increase of the surface area and enhanced response under mechanical stress, while cerium doping was employed to regulate defect levels within the  $\text{BaTiO}_3$  lattice. As shown in Fig. 11a, this modification led to a significant enhancement of the piezoelectric response from 0.13 to 0.89 V and improved efficiency in converting mechanical stress into electrical energy, leading to a substantial increase in the antibacterial activity, with over 90% reduction in bacterial viability for *E. coli* and *S. aureus* under piezoelectric activation. Notably, both  $\text{BaTiO}_3$  and  $\text{hBT}_{\text{Ce}}$  nanoparticles were strongly piezoelectric and the enhanced production of ROS by  $\text{hBT}_{\text{Ce}}$  under sonication led to significant destruction of bacterioplankton and biofilms (Fig. 11b).

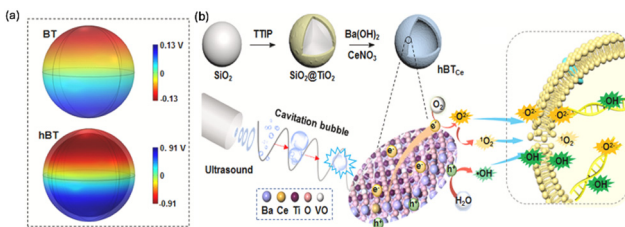


Fig. 11 Synthesis and piezocatalytic activity of the BaTiO<sub>3</sub> (BT) and hBT<sub>Ce</sub> nanoparticles. (a) Piezoelectric property. (b) Schematic illustration of the preparation process and antibacterial mechanism of the hBT<sub>Ce</sub> nanoparticles. Reproduced with permission from ref. 64, copyright 2023, Elsevier.

These results highlight the effectiveness of the structural design and defect engineering in enhancing the antibacterial performance of BaTiO<sub>3</sub> nanoparticles.

#### 4.4. Metal-organic frameworks

Metal-organic frameworks (MOFs) are another family of promising materials for piezocatalytic antibacterial applications due to their unique structural properties, high surface area, and tunable functionalities. Recent studies have demonstrated the efficacy of MOFs, such as zeolitic imidazolate framework-8 (ZIF-8), Material Institute Lavoisier-53 with iron (MIL-53(Fe)), zinc-based metal-organic frameworks (Zn-MOFs), and cobalt-based metal-organic frameworks (Co-MOFs), in generating ROS under mechanical stress, leading to effective bacterial inactivation.<sup>65</sup> For instance, ZIF-8, when subjected to ultrasonic vibration, exhibited a piezoelectric coefficient of about 2.5 pC N<sup>-1</sup>, generating substantial amounts of hydroxyl radicals and superoxide ions that disrupted bacterial cell membranes.<sup>62,66</sup> Zhu *et al.*<sup>53</sup> prepared a dynamically evolving antibacterial and repair-promoting BTO@ZIF-8/CIP nanocomposite by *in situ* self-assembly of ZIF-8 onto the surface of barium titanate (BaTiO<sub>3</sub>) and further modification with a small amount of ciprofloxacin (CIP). ROS was generated through sono-dynamic processes, resulting in a synergistic antibacterial effect

with an inhibition rate exceeding 99.9%. As shown in Fig. 12a-d, treatment with BaTiO<sub>3</sub> at a concentration of 50 µg mL<sup>-1</sup> alone did not result in significant damage to *S. aureus*. A marginal increase in bacterial mortality was observed by ultrasonic irradiation alone for 5 min, which was attributed to mechanical damage and inertial acoustic cavitation effects induced by the ultrasound. However, when BaTiO<sub>3</sub> (50 µg mL<sup>-1</sup>) was subjected to ultrasonic treatment, the survival rate of *S. aureus* was reduced to 55%, indicating effective production of ROS by the piezoelectric BaTiO<sub>3</sub> nanoparticles that effectively kill bacteria.

Due to the high specific surface area and rich active sites of the MOF materials, they are often used as carriers and combined with other piezoelectric materials to further improve the piezocatalytic sterilization performance.<sup>65,66</sup> Ruan *et al.*<sup>66</sup> synthesized ZIF-8 nanoparticles using a liquid-phase method and observed an exceptional piezoelectric catalytic performance. As illustrated in Fig. 13, the ZIF-8 nanoparticles exhibited a dodecahedral morphology with a porous surface structure, and a broad range of piezoelectric hysteresis loops.

In addition, Chen *et al.*<sup>67</sup> integrated ZIF-8 into a hierarchical polyvinylidene fluoride (PVDF) piezoelectric foam nanogenerator to enhance the piezocatalytic and antibacterial properties. The piezoelectric coefficient of ZIF-8 was about 2.4 pC N<sup>-1</sup>, which enabled the nanocomposites to effectively generate ROS under mechanical stress. As a result, the antibacterial inhibition rate against *E. coli* and *S. aureus* was significantly improved, reaching a piezoelectric sterilization efficiency of about 90% (Fig. 14).

For the application of piezoelectric materials as antibacterial agents, in general, the higher the piezoelectric performance, the better the sterilization effect. Therefore, piezoelectric ceramics with an ultrahigh piezoelectric catalytic response have more significant advantages, but they also have the limitation of harsh synthesis conditions and difficulty in compounding with other materials at relatively low reaction temperatures.<sup>59</sup> Although the piezoelectric response of transition metal sulfides is limited, it is dependent on the number of layers, and the

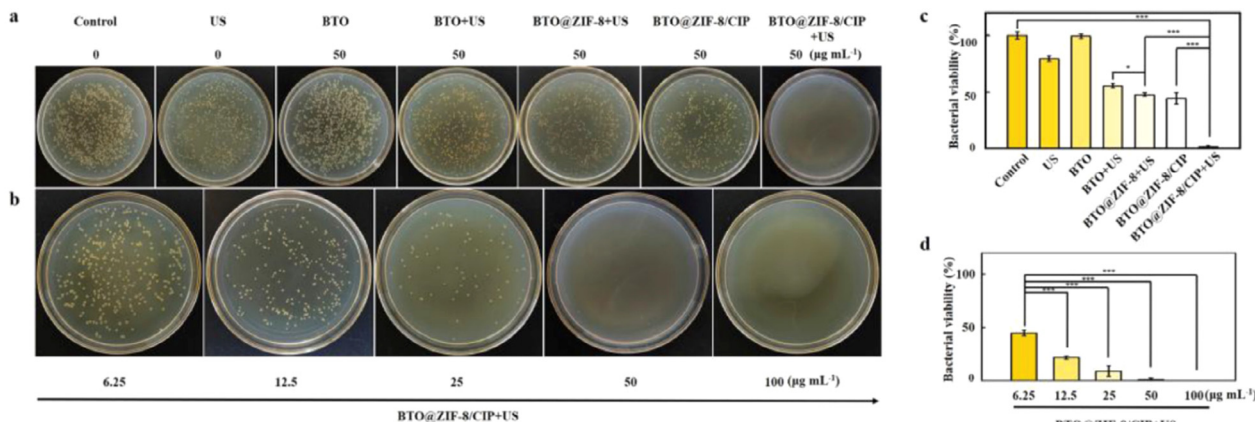


Fig. 12 Antibacterial activity of BTO@ZIF-8/CIP nanocomposites. (a) Photographs of *S. aureus* colonies in agar plates after different treatments. (b) Photographs of *S. aureus* colonies in agar plates treated by US irradiation with different concentrations of BTO@ZIF-8/CIP nanocomposites. (c) and (d) Summary of bacterial activities after treatments as in (a) and (b). Reproduced with permission from ref. 53, copyright 2023, Elsevier.

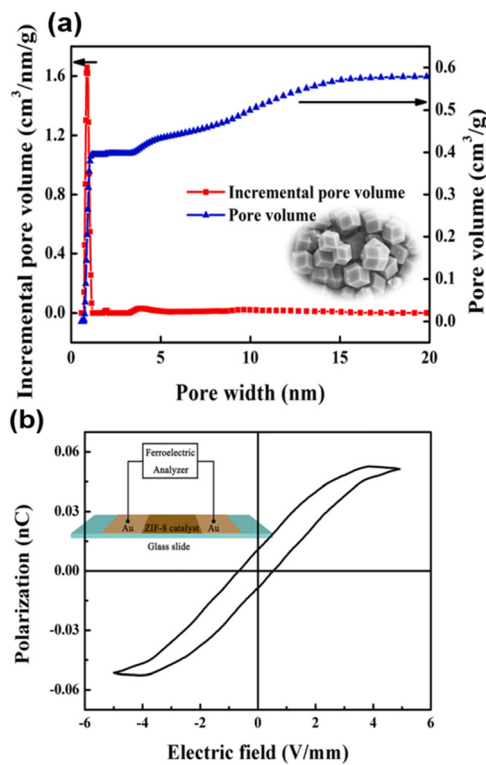


Fig. 13 Porosity and ferroelectric property of ZIF-8. (a) Distribution of pore volume with pore diameter of ZIF-8. Inset is an SEM image of the sample. (b) Ferroelectric hysteresis loop of ZIF-8. Inset is a schematic diagram for the piezoelectric measurement. Reproduced with permission from ref. 66, copyright 2023, Elsevier.

piezoelectric response can be improved by structural regulation. At the same time, they have relatively mild synthesis conditions and have good application prospects in piezoelectric sterilization, but it is necessary to point out that sulfur may provide sites for the growth of bacterial colonies and compromise the sterilization efficiency.<sup>56</sup> Piezoelectric polymers have good application prospects in the field of piezoelectricity and can be compounded with most inorganic piezoelectric materials to improve the application scope and scenarios of piezoelectric sterilization. However, how to avoid bacterial contamination of the organic components of the polymers is also an issue that needs to be considered in research. In general, it is necessary to select a piezoelectric material according to the structural characteristics and the application scenarios. The complementary advantages of the strong coupling of multiple materials may be an important research direction.

## 5. Enhancement strategies of piezocatalytic antibacterial efficiency

### 5.1. Formation of heterostructures

The formation of heterostructures has emerged as a viable strategy to further enhance the antibacterial performance of piezoelectric catalysts. By combining different materials with complementary properties, heterostructures can effectively optimize electron transfer and enhance the generation of ROS, which are crucial for bactericidal activity.<sup>20,53,67-69</sup> For instance, Yu *et al.*<sup>70</sup> designed an ultrasound-activated

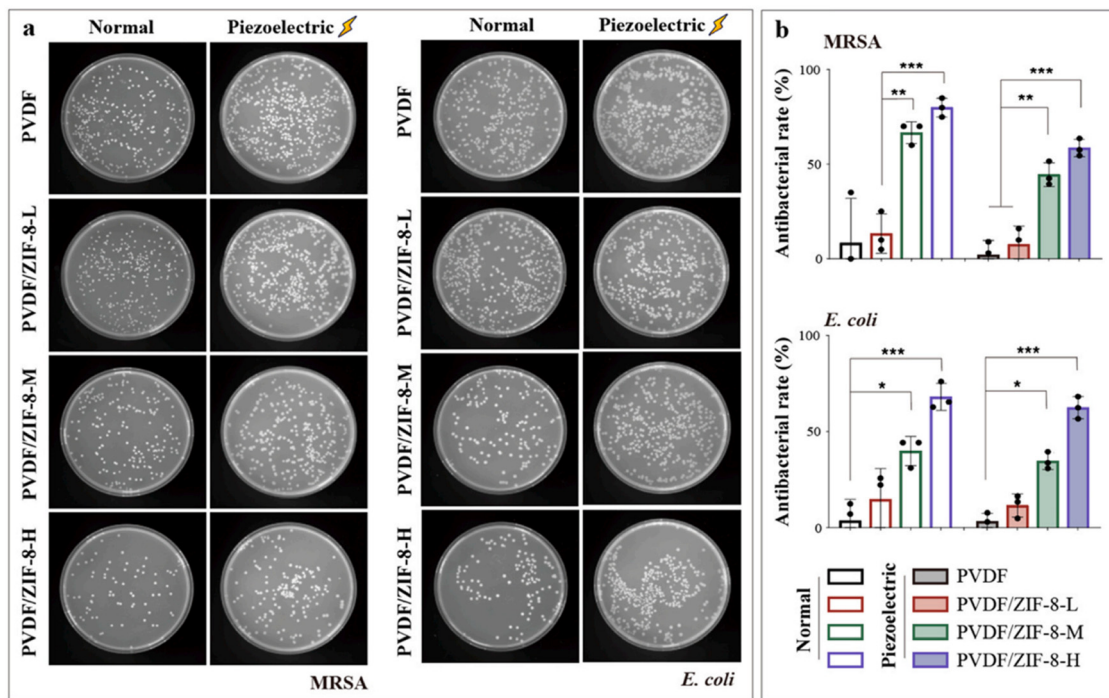


Fig. 14 Antibacterial effect of PVDF/ZIF-8 foam-based piezoelectric sheets. (a) Plate photographs of the colonies formed by MRSA and *E. coli* under normal and piezoelectric conditions after 24 h. (b) Bar graphs show the antibacterial rate of PVDF and PVDF/ZIF-8 groups under normal and piezoelectric conditions after 24 h ( $n = 3$ ). Reproduced with permission from ref. 67, copyright 2023, Elsevier.

piezoelectric responsive heterojunction (PCN-222-BTO, with PCN-222 being a porphyrin metal-organic framework) that can change the electron transfer pathway at the abiotic and abiotic-biotic interfaces under the action of ultrasound, thereby achieving a rapid (15 min) and highly efficient bactericidal effect with a bactericidal efficacy up to 99.96% (Fig. 15a and b). The specific mechanism in Fig. 15c showed that after PCN-222 was compounded with BTO, the built-in electric field generated by BTO under the action of ultrasound promoted the transfer of electrons at the PCN-222-BTO interface, BTO was depolarized, and the electrons on PCN-222 were released and reacted with  $O_2$  to generate singlet oxygen ( $^1O_2$ ) and  $O_2^{\bullet-}$ , thereby improving the piezocatalytic activity of PCN-222. Pan *et al.*<sup>69</sup> applied doped piezoelectric nanocoatings ( $g_{33} = 13.8 \text{ pm V}^{-1}$ ) on dental implants, and observed an improved antimicrobial efficiency, with more than 90% reductions of the *S. aureus* and *E. coli* counts under ultrasound stimulation, as compared to less than 50% for the undoped coatings. This was attributed to the creation of heterojunctions, which facilitated charge separation and ROS generation. In addition, the doped nanocoatings enhanced osteogenic activity, with a 35% increase of the alkaline phosphatase activity and a 25% increase of mineral deposition in osteoblast cultures, as compared to the control samples. These findings suggest that the construction of heterojunctions can significantly improve the

piezoelectric properties and bactericidal activity of piezoelectric materials by narrowing the band gap and strengthening the mechanical response.

## 5.2. Doping and compositing

Doping represents an instrumental strategy in enhancing the piezoelectric properties of materials by modifying the structural and electronic characteristics. The modifications can result in an increased density of oxygen vacancies and the formation of local electric fields, which collectively enhance the piezoelectric effect. The presence of dopants can also induce lattice distortions that augment polarization and improve the mechanical properties of the material, leading to an amplified piezoelectric response.<sup>71-76</sup> In particular, when metal ions that are bactericidally active (such as silver, copper, zinc, *etc.*) are doped into a material matrix,<sup>72</sup> the ions can cause bacterial death or inhibit growth by reacting with proteins and enzymes in the bacterial cells. For instance, Wang *et al.*<sup>77</sup> prepared a series of Cu-doped ZIF-8 and observed antimicrobial activity against bacteria like *E. coli* and *S. aureus* in the dark, due to effective ROS generation (Fig. 16a). In another study (Fig. 16b), Han *et al.*<sup>73</sup> prepared Ba-doped brookite  $TiO_2$  nanorods ( $TiO_2$ :Ba) and observed that the lattice distortion-induced polarization and vacancy defect engineering increased ROS production and achieved a 100% inhibition rate even at low doses against *E. coli*.

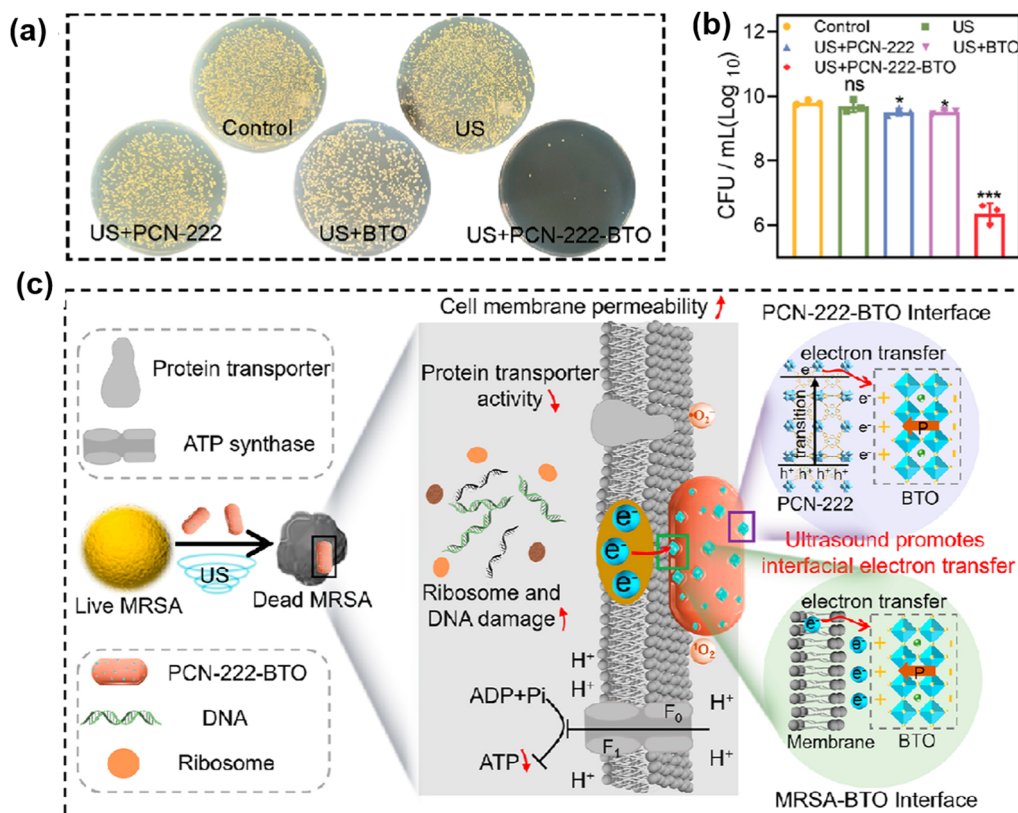


Fig. 15 *In vitro* antibacterial performance: (a) spread plate and (b) number of MRSA colonies after treatments with different piezocatalysts in the absence and presence of ultrasound (US). (c) Mechanism of ultrasound-promoted interfacial electron transfer in the heterostructure. Reproduced with permission from ref. 70, copyright 2023, American Chemical Society.

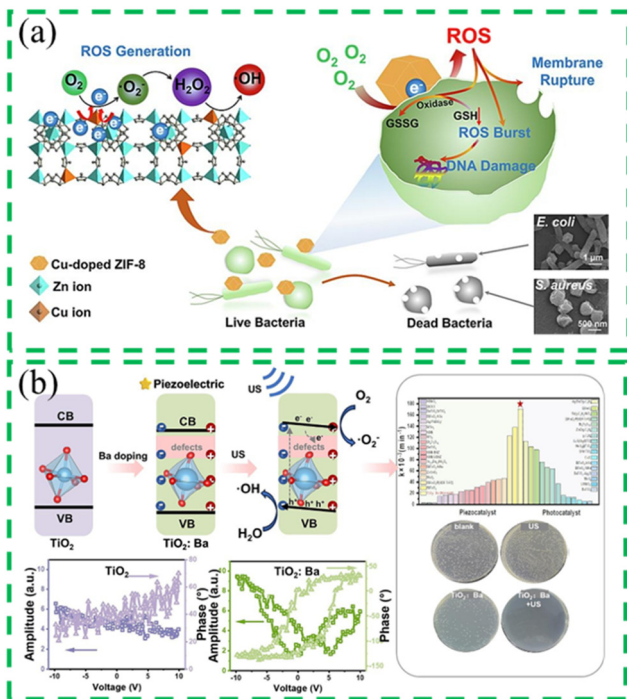


Fig. 16 (a) Cu-doped ZIF-8 bactericidal mechanism diagram. Reproduced with permission from ref. 77, copyright 2023, Elsevier. (b) TiO<sub>2</sub> and TiO<sub>2</sub>: Ba degradation mechanism and bactericidal effect comparison diagram. Reproduced with permission from ref. 73, copyright 2024, Elsevier.

The compositing strategy is another important method to improve the piezoelectric properties of materials, due to interfacial charge regulation, stress transfer, and polarization enhancement through the synergistic interactions between multiphase materials. In recent years, research has mainly focused on inorganic–inorganic composites, inorganic–organic composites, and nanocomposites.<sup>71–76</sup> For instance, Fu *et al.*<sup>74</sup> doped barium hydroxylated titanate (BT-OH) nanoparticles and MXene into chitosan/bacterial cellulose (CB) aerogel to prepare biomass aerogel composites, which exhibited excellent piezoelectric and photothermal antibacterial properties, achieving a complete bactericidal effect against *S. aureus* and *E. coli*. Liu *et al.*<sup>78</sup> prepared a series of piezoelectric catalysis composites using poly(L-lactic acid) (PLLA), poly(ethylene glycol) (PEG) and tetragonal barium titanate (BT). During the initial treatment stage, the piezoelectricity of the as-prepared composites (PLE-BT NFM) exhibited apparent piezoelectric properties, with a  $d_{33}$  coefficient at *ca.* 10 pC N<sup>-1</sup>, significantly higher than conventional biodegradable materials (around 2–4 pC N<sup>-1</sup>). This enhancement in piezoelectric performance enabled the composites to generate electrical charges when subjected to mechanical deformation, such as from body movements. The electrical stimulation further increased the generation of ROS, leading to a notable antibacterial efficiency of around 95% against pathogens like *S. aureus* and *E. coli*, as compared to less than 60% in non-piezoelectric fibrous composites. The improved piezoelectric properties were ascribed to the integration of doped materials that formed heterojunctions, facilitated charge separation and increased ROS generation. These active

substances affected the bacteria's energy production and synthesis of important molecules, leading to bacterial cell death.

### 5.3. Rigid-flexible structural coupling

The rigid-flexible structure coupling strategy is a material design and manufacturing method that combines materials with different mechanical hardness/stiffness to optimize performance and function.<sup>76,77,79</sup> The core of this strategy is to exploit the complementary advantages of different materials, thereby creating a composite structure that is both rigid and flexible. The rigid-flexible structure coupling strategy in sterilization applications mainly refers to the combination of rigid materials with sterilization functions and flexible and adsorbent materials to enhance the sterilization effect and improve the functionality and durability of the material.<sup>80</sup> For example, Wang *et al.*<sup>81</sup> introduced rigid ZnO nanoparticles into flexible PVDF, thereby increasing the piezoelectric response of PVDF by 6 times (from 5.8 to 34.7 mV). As shown in Fig. 17a–d, the prepared nanocomposite showed an excellent bactericidal performance against *E. coli*, with more than 98% elimination after treatment with a water flow at 0.5 m s<sup>-1</sup> for 30 min. They also found that the rigid-flexible structure not only improved the piezoelectric response but also improved the mechanical sensitivity of PVDF. Similarly, as shown in Fig. 17e, Huo *et al.*<sup>79</sup> also found that introducing rigid MoS<sub>2</sub> nanosheets into PVDF significantly improved the piezoelectric properties and mechanical force sensitivity of PVDF, resulting in a piezoelectric coefficient of *ca.* 12.8 pC N<sup>-1</sup>. This enhancement significantly boosted the efficiency of antibiotic degradation while reducing energy consumption compared to conventional materials.

### 5.4. Piezo-photocatalytic coupling

Piezoelectric-photocatalytic coupling can also markedly enhance the antibacterial efficacy by utilizing both light and mechanical energy (such as pressure and vibration) to effectively drive the antibacterial processes,<sup>82</sup> so as to generate highly reactive radicals and rapidly disrupt microbial cell walls, thereby facilitating efficient bacterial eradication. Additionally, this technology offers environmental benefits by reducing reliance on conventional chemical disinfectants and minimizing associated pollution. Its high selectivity and robust resistance to contamination ensure sustained antibacterial activity over time. Furthermore, the technology's low energy consumption renders it a cost-effective and practical solution for diverse applications.

As shown in Fig. 18, Xuan *et al.*<sup>83</sup> proposed a controllable defect engineering strategy to stimulate the piezoelectric response of ReS<sub>2</sub>. The introduction of vacancy defects led to the removal of the initial centrosymmetric structure, thereby breaking the piezoelectric polarization bonds and generating piezoelectric properties. The optimized ReS<sub>2</sub>@C-40 materials featured a  $g_{33}$  coefficient of 23.07 pm V<sup>-1</sup>, promoted the separation of photoexcited carriers and endowed ReS<sub>2</sub>@C-40 with efficient piezoelectric-photocatalytic synergistic bactericidal properties. Within 30 min, the material eradicated 99.99% of *E. coli* and 96.67% of *S. aureus*.

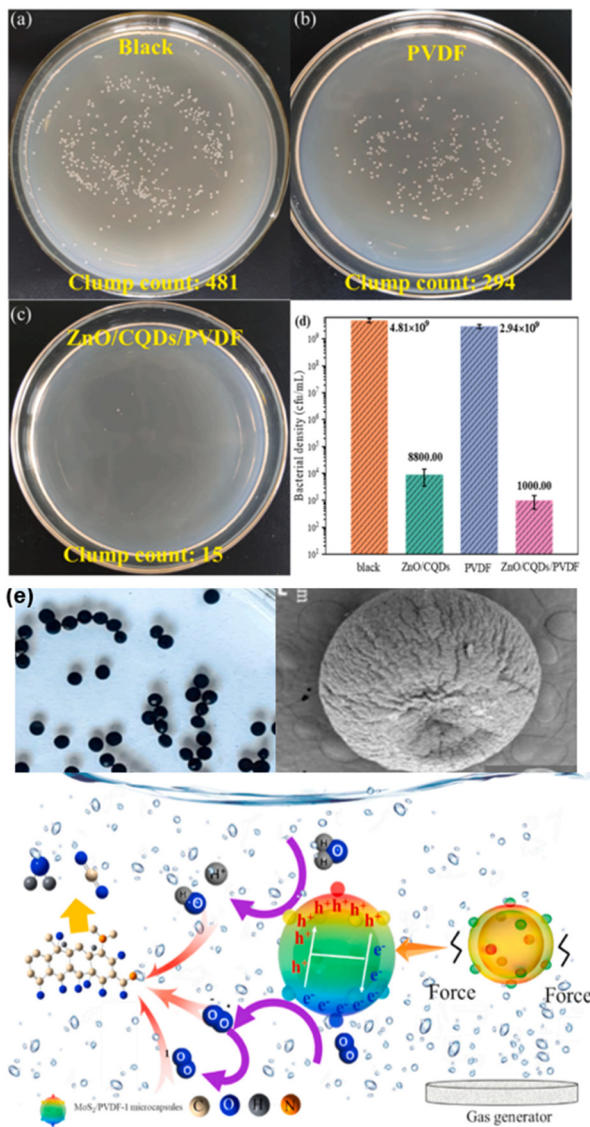


Fig. 17 Piezocatalytic activity of ZnO/CQDs/PVDF composites. Photographs of *E. coli* cultured for 12 h in the presence of (a) the control, (b) PVDF, and (c) ZnO/CQDs/PVDF. (d) The corresponding bacterial density. Reproduced with permission from ref. 81, copyright 2023, Elsevier. (e) Mechanism of the piezocatalytic generation of oxygen radicals from MoS<sub>2</sub>/PVDF microcapsules. Reproduced with permission from ref. 79, copyright 2023, Elsevier.

Kumar *et al.*<sup>80</sup> studied the effect of BaTiO<sub>3</sub> ceramic piezoelectric photocatalysis on bacterial degradation. At a frequency of 8 Hz, the BaTiO<sub>3</sub> ceramic produced an open circuit peak-to-peak voltage of 1.4 V, which facilitated the decomposition of water molecules and generation of ROS, leading to bacterial inactivation. Indeed, complete elimination of *E. coli* was achieved within 30 min's ultrasound treatment.

### 5.5. Piezoelectric Fenton strategy

The piezo-Fenton method is a major advance in environmental remediation that combines piezocatalysis with Fenton-like reactions to enhance the degradation of organic pollutants.<sup>84,85</sup> This method

exploits the piezoelectric effect, where mechanical stress or vibration generates charges in piezoelectric materials, which activate Fenton reactions. These reactions involve the generation of hydroxyl radicals through the reaction of hydrogen peroxide with an iron-based catalyst. Recent studies have shown that the piezoelectric process in the piezo-Fenton system can promote the electron transfer of the Fenton process, while the Fenton process facilitates the migration of electrons/holes in the piezoelectric process, thereby improving the efficiency of active species generation.<sup>86-88</sup>

The piezoelectric Fenton method is widely used in the treatment of organic pollutants, but there is relatively scarce research on sterilization applications. Recently, Chai *et al.*<sup>84</sup> studied how the piezoelectric field generated by poly(vinylidene fluoride)-hexafluoro propylene under the action of flowing water helped promote the piezoelectric-Fenton reaction of Fe<sub>2</sub>O<sub>3</sub>/PVDF-HFP porous membranes towards the degradation of tetracycline, a common antibiotic. After 11 h of stirring, 53.7% of tetracycline was degraded. Compared with the pure PVDF-HFP porous membrane, the degradation rate of Fe<sub>2</sub>O<sub>3</sub>/PVDF-HFP porous membrane increased by about 37 times, due primarily to the formation of O<sub>2</sub><sup>•-</sup>. α-Fe<sub>2</sub>O<sub>3</sub> nanoparticles enhanced the piezoelectric catalytic performance of PVDF-HFP through the β phase, and promoted the reaction of Fe<sup>3+</sup> with H<sub>2</sub>O<sub>2</sub> generated by the piezoelectric membrane, triggering additional Fenton reactions (Fig. 19). In addition, the piezoelectric field accelerated the cycle of Fe<sup>3+</sup>/Fe<sup>2+</sup> in the Fenton reaction, further promoting the progress of the Fenton reaction.

Xu *et al.*<sup>85</sup> developed a Fe<sup>III</sup>/BiOIO<sub>3</sub> piezoelectric catalytic Fenton system with strong oxidation ability and efficient pollutant degradation. This system exhibited an extremely high activity towards two-electron water oxidation to H<sub>2</sub>O<sub>2</sub> without the addition of any sacrificial reagents. As shown in Fig. 20, the added Fe not only continuously provided the Fe required for the Fenton reaction, but also promoted the generation of H<sub>2</sub>O<sub>2</sub>. These two together promoted a significant Fenton degradation effect in the Fe<sup>III</sup>/BiOIO<sub>3</sub> system, demonstrating a faster Fe<sup>III</sup>/Fe<sup>II</sup> cycle rate, a higher OH yield and a stronger pollutant degradation ability, as compared to the traditional BIO/Fe piezoelectric catalytic Fenton system.

In addition, Ge *et al.*<sup>89</sup> observed enhanced antibacterial activity of piezoelectric Fe-doped g-C<sub>3</sub>N<sub>4</sub> *via* a Fenton-like reaction. They found that the piezoelectrically induced generation of electrons on the g-C<sub>3</sub>N<sub>4</sub> matrix facilitated the conversion of Fe(III) to Fe(II) and promoted the rate-limiting step of the Fenton reaction, thereby improving the bactericidal efficiency. Under ultrasonic stimulation, the system exhibited notable bactericidal effects against *E. coli* and *S. aureus*, achieving a sterilization efficiency of 75% and 80% within 60 min, respectively. This bactericidal performance was attributed to the synergistic action of highly reactive free radicals, which played a key role in disrupting bacterial cell structures, and the increased permeability of cell membranes that facilitated the entry of reactive species into the cells.

Among the various strategies for improving the piezoelectric antibacterial performance, each entails a different synthesis method and distinct characteristics, and its application range

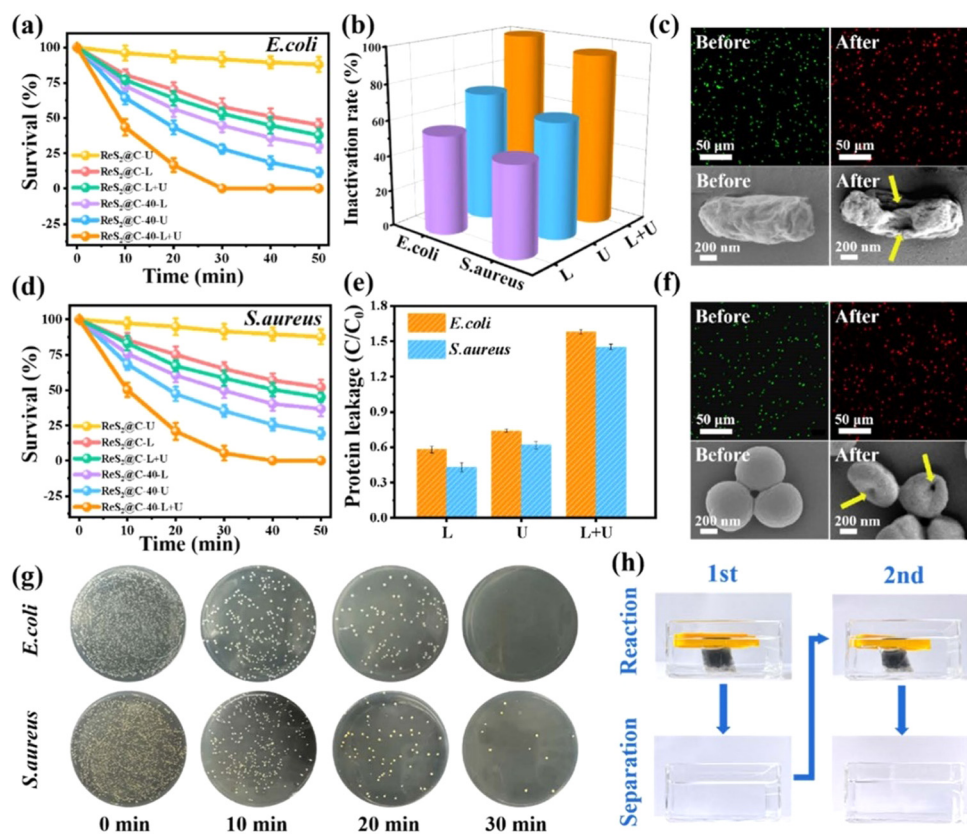


**Fig. 18** Sterilization performance of  $\text{ReS}_2@\text{C}$  and  $\text{ReS}_2@\text{C-40}$  against (a) *E. coli* and (d) *S. aureus*. (b) Inactivation rate and (e) protein leakage of  $\text{ReS}_2@\text{C-40}$  under different conditions for 30 min. CLSM images of live/dead-stained bacteria and SEM images of (c) *E. coli* and (f) *S. aureus* before or after treatment with  $\text{ReS}_2@\text{C-40}$  under light and ultrasound for 30 min. (g) Results of the spread plate test of  $\text{ReS}_2@\text{C-40}$  under light and ultrasound. (h) Schematic representation of the recycling device. (L: light, U: ultrasonic, L + U: light and ultrasonic). Reproduced with permission from ref. 83, copyright 2023, American Chemical Society.

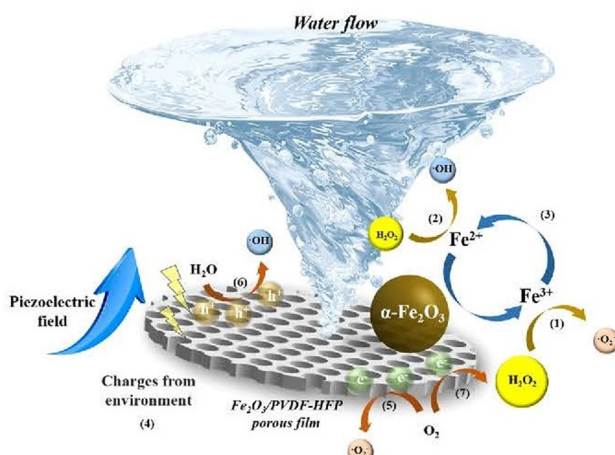


**Fig. 19** Mechanism of piezo-Fenton catalysis by a  $\text{Fe}_2\text{O}_3/\text{PVDF-HFP}$  porous film. Reproduced with permission from ref. 84, copyright 2022, Elsevier.

is also different. Specifically, heterostructures optimize the interface properties and electron-transfer efficiency by coupling different piezoelectric materials, and improve the

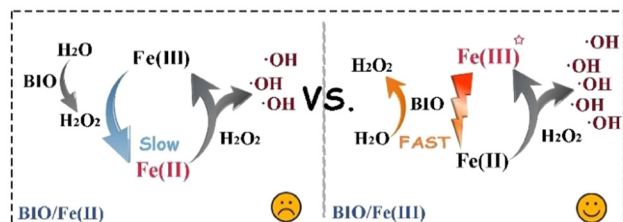


**Fig. 20** Mechanisms of enhanced oxidation capacity in the  $\text{BIO/Fe}^{3+}$  system. Reproduced with permission from ref. 85, copyright 2023, Wiley.

overall piezoelectric catalytic performance.<sup>87</sup> It is suitable for catalytic antibacterial reactions that require efficient electron-hole separation and rapid electron transfer. The doping strategy adjusts the electronic structure and band structure of the material by introducing specific impurity elements, while enhancing the piezoelectric and catalytic activity. It is more suitable for piezocatalytic antibacterial reactions that require manipulation of the electronic structure of the material to improve the reaction activity, especially in high-temperature, high-pressure or corrosive environments. Rigid-flexible structure coupling has both flexibility and high piezoelectric

performance and is suitable for dynamic and real-time antibacterial environments. Piezoelectric-photocatalytic coupling can significantly enhance the antibacterial effect under illumination, but is limited by light source conditions.<sup>88</sup> The piezoelectric-Fenton strategy uses mechanical stress and Fenton reaction to generate highly oxidative free radicals, which is applicable to a wider pH range and can maintain effective antibacterial performance even in acidic environments. Therefore, in practical applications, researchers can choose the appropriate method based on the characteristics of each method and the performance of the material.

## 6. Summary and perspectives

In recent years, with advancements in the design and engineering of piezoelectric materials, piezocatalytic antibacterial applications have emerged as a new area of interest.<sup>7–12,35</sup> Unlike traditional antibacterial methods, piezocatalytic antibacterial agents offer several unique advantages, including the absence of added oxidants, no residual byproducts, and ease of operation under light-free and electrolyte-free conditions. These characteristics suggest significant potential for applications in water treatment, medical sterilization, food sterilization, and general disinfection.<sup>90</sup> Furthermore, recent innovations in piezoelectric material design, such as defect engineering and formation of heterojunctions, have greatly boosted the development of piezoelectric materials for antibacterial applications.

Despite the progress, key challenges remain, in particular, in optimizing the properties of piezoelectric materials and expanding their applications. Addressing these challenges is critical to advancing the practical application and effectiveness of the piezocatalytic antibacterial technology.

(a) The low piezoelectric coefficients of most reported piezoelectric materials restrict their antibacterial activity. The piezoelectric coefficients ( $d_{33}$ ) for commonly used materials and their modified materials are typically in the range of 1–100 pC N<sup>−1</sup>, which may be insufficient for antibacterial applications. Future research should focus on structural design strategies to enhance the piezoelectric efficiency by, for instance, optimizing the microstructure and introducing defects, so as to improve the piezoelectric antibacterial activity.

(b) The utilization rate of mechanical force in piezoelectric catalysis remains limited. Research is therefore desired to optimize the conversion efficiency of mechanical energy into piezoelectric responses. In fact, the low conversion efficiency of mechanical energy into piezoelectricity limits the production of ROS and other antibacterial agents. Improving the efficiency of piezoelectric energy conversion can lead to a higher yield of active species.

(c) Although studies have demonstrated that piezoelectric catalysts have significant potential for inhibiting bacterial growth, the mechanisms by which piezoelectric materials exert antibacterial effects have not been fully understood thus far. While ROS and cell membrane disruption are identified as the key contributors, the precise interactions between piezoelectric

charges and bacterial cells need further investigation. In particular, the synergistic effects in the piezoelectric catalytic process, such as thermal effects, magnetic effects, and high-pressure interfaces, and their inhibitory effects on bacterial growth and reproduction have not been thoroughly studied. Understanding these mechanisms at the molecular level will facilitate targeted material design and improve the antibacterial efficacy.

(d) Material stability and recyclability present significant challenges in practical applications. Most piezoelectric catalytic materials are in powder form, which complicates device fabrication and system integration. Issues such as device molding, powder recovery, and incorporation of powders into functional devices need to be addressed. Ensuring long-term stability under mechanical stress and diverse environmental conditions is also critical. For example, piezoelectric ceramics often experience a reduction in performance to 70–80% of their initial capability after just 5 mechanical cycles. Structural damage resulting from mechanical force can affect the material's catalytic stability and longevity, necessitating strategies to enhance the structural integrity. Furthermore, developing recycling methods that maintain both activity and piezoelectric properties of the materials is essential for sustainable use. Overcoming these challenges is crucial for the effective application of piezoelectric catalytic materials.

The methodologies discussed herein are beneficial for enhancing the sterilization efficiency of piezoelectric catalytic materials and offer novel directions for their design and antibacterial application. This review aims to provide guidance and references for the development of efficient piezoelectric catalytic materials for practical applications, as well as to advance our understanding of the piezocatalytic antibacterial mechanisms. It is anticipated that piezocatalytic sterilization will play an increasingly active role in practical applications and in mitigating bacterial resistance.

## Author contributions

Fanqing Meng: investigation, funding acquisition, writing – original draft; Chenxi Guo: investigation, writing – original draft; Tianchen Cui: investigation, writing – original draft; Mingyang Xu: investigation; Xiaxia Chen: investigation; Hongwei Xu: investigation; Chao Liu: investigation; Shaowei Chen: conceptualization, investigation, funding acquisition, writing – review & editing.

## Data availability

The data that support the findings of this study are available from the corresponding author upon reasonable request.

## Conflicts of interest

There are no conflicts to declare.

## Acknowledgements

This work was supported by the Natural Science Foundation of China (NSFC 52400041 and 52372212) and the US National Science Foundation (CHE-2003685).

## References

- J. Hasan, R. J. Crawford and E. P. Ivanova, Antibacterial surfaces: the quest for a new generation of biomaterials, *Trends Biotechnol.*, 2013, **31**, 295–304.
- A. M. Kraigsley and S. E. Finkel, Adaptive evolution in single species bacterial biofilms, *FEMS Microbiol. Lett.*, 2009, **293**, 135–140.
- M. Santosham, A. Chandran, S. Fitzwater, C. Fischer-Walker, A. H. Baqui and R. Black, Progress and barriers for the control of diarrhoeal disease, *Lancet*, 2010, **376**, 63–67.
- Y. Wang, K.-K. Liu, W.-B. Zhao, J.-L. Sun, X.-X. Chen, L.-L. Zhang, Q. Cao, R. Zhou, L. Dong and C.-X. Shan, Antibacterial fabrics based on synergy of piezoelectric effect and physical interaction, *Nano Today*, 2023, **48**, 101737.
- M. Klausen, M. Ucuncu and M. Bradley, Design of Photosensitizing Agents for Targeted Antimicrobial Photodynamic Therapy, *Molecules*, 2020, **25**, 5239.
- D. Şen Karaman, U. K. Ercan, E. Bakay, N. Topaloğlu and J. M. Rosenholm, Evolving Technologies and Strategies for Combating Antibacterial Resistance in the Advent of the Postantibiotic Era, *Adv. Funct. Mater.*, 2020, **30**, 1908783.
- A. Bharadwaj, A. Rastogi, S. Pandey, S. Gupta, J. S. Sohal and S. Kaushik, Multidrug-Resistant Bacteria: Their Mechanism of Action and Prophylaxis, *BioMed Res. Int.*, 2022, **2022**, 1–17.
- M. Gong, S. Xiao, X. Yu, C. Dong, J. Ji, D. Zhang and M. Xing, Research progress of photocatalytic sterilization over semiconductors, *RSC Adv.*, 2019, **9**, 19278–19284.
- C. Ai, X. Wu, Y. Ke, Y. Lei and X. Shao, Synthesis and Photocatalytic Sterilization Performance of SA/TiO<sub>2</sub>, *J. Inorg. Organomet. Polym. Mater.*, 2020, **30**, 3378–3387.
- X. Q. Pan, W. Y. Dong, J. S. Zhang, Z. X. Xie, W. Li, H. R. Zhang, X. J. Zhang, P. H. Chen, W. Y. Zhou and B. F. Lei, TiO<sub>2</sub>/Chlorophyll S-Scheme Composite Photocatalyst with Improved Photocatalytic Bactericidal Performance, *ACS Appl. Mater. Interfaces*, 2021, **13**, 39446–39457.
- G. Cheng, Z. Li, L. Sun, Y. Li and J. Fu, Application of Microwave/Electrodeless Discharge Ultraviolet/Ozone Sterilization Technology in Water Reclamation, *Process Saf. Environ. Prot.*, 2020, **138**, 148–156.
- R. Sommer, W. Pribil, S. Pfleger, T. Haider, M. Werderitsch and P. Gehringer, Microbicidal efficacy of an advanced oxidation process using ozone/hydrogen peroxide in water treatment, *Water Sci. Technol.*, 2004, **50**, 159–164.
- M. Zhu, B. Liao, Y. Tang, X. Chen, R. Ma, L. Li and X. Fan, The superior piezocatalytic performance of SrBi<sub>2</sub>Ta<sub>2</sub>O<sub>9</sub> nanoflower: Mechanism of screening effect and energy band theory, *Appl. Surf. Sci.*, 2023, **628**, 157366.
- C. Wang, W. Sun, Y. Xiang, S. Wu, Y. Zheng, Y. Zhang, J. Shen, L. Yang, C. Liang and X. Liu, Ultrasound-Activated Piezoelectric MoS<sub>2</sub> Enhances Sonodynamic for Bacterial Killing, *Small Sci.*, 2023, **3**, 2300022.
- S. Lan, X. Ke, Z. Li, L. Mai, M. Zhu and E. Y. Zeng, Piezoelectric disinfection of water co-polluted by bacteria and microplastics energized by water flow, *ACS ES&T Water*, 2022, **2**, 367–375.
- Q. Lian, W. Liu, D. Ma, Z. Liang, Z. Tang, J. Cao, C. He and D. Xia, Precisely orientating atomic array in one-dimension tellurium microneedles enhances intrinsic piezoelectricity for an efficient piezo-catalytic sterilization, *ACS Nano*, 2023, **17**, 8755–8766.
- X. Yang, Z. Yang, X. Wang, Y. Guo, Y. Xie, W. Yao and H. Kawasaki, Piezoelectric nanomaterials for antibacterial strategies, *Appl. Mater. Today*, 2024, **40**, 102419.
- X. Zhang, Z. Yang, J. Zhang, L. Wang, M. Zhou, N. Ren, L. Ding, A. Wang, Z. Wang, H. Liu and X. Yu, Piezotronic effect enhanced catalytic sterilization: Mechanisms and practical applications, *Nano Energy*, 2024, **131**, 110346.
- F. Bößl, V. C. Menzel, K. Jeronimo, A. Arora, Y. Zhang, T. P. Comyn, P. Cowin, C. Kirk, N. Robertson and I. Tudela, Importance of energy band theory and screening charge effect in piezo-electrocatalytical processes, *Electrochim. Acta*, 2023, **462**, 142730.
- Z. Ren, F. Chen, Q. Zhao, G. Zhao, H. Li, W. Sun, H. Huang and T. Ma, Efficient CO<sub>2</sub> reduction to reveal the piezocatalytic mechanism: From displacement current to active sites, *Appl. Catal., B*, 2023, **320**, 122007.
- N. Meng, W. Liu, R. Jiang, Y. Zhang, S. Dunn, J. Wu and H. Yan, Fundamentals, advances and perspectives of piezocatalysis: A marriage of solid-state physics and catalytic chemistry, *Prog. Mater. Sci.*, 2023, 101161.
- P. Puneetha, S. P. R. Mallem, P. Bathalavaram, J.-H. Lee and J. Shim, Temperature dependence of the piezotronic effect in CdS nanospheres, *Nano Energy*, 2021, **84**, 105923.
- Y. Sun, S. Shen, W. Deng, G. Tian, D. Xiong, H. Zhang, T. Yang, S. Wang, J. Chen and W. Yang, Suppressing piezoelectric screening effect at atomic scale for enhanced piezoelectricity, *Nano Energy*, 2023, **105**, 108024.
- C. Chen, X. Wang, Y. Wang, D. Yang, F. Yao, W. Zhang, B. Wang, G. A. Sewwandi, D. Yang and D. Hu, Additive manufacturing of piezoelectric materials, *Adv. Funct. Mater.*, 2020, **30**, 2005141.
- M.-M. Yang, T.-Y. Zhu, A. B. Renz, H.-M. Sun, S. Liu, P. M. Gammon and M. Alexe, Auxetic piezoelectric effect in heterostructures, *Nat. Mater.*, 2024, **23**, 95–100.
- H. Li, J. Zhao, Y. Li, L. Chen, X. Chen, H. Qin, H. Zhou, P. Li, J. Guo and D. Wang, Bismuth Ferrite-Based Lead-Free High-Entropy Piezoelectric Ceramics, *ACS Appl. Mater. Interfaces*, 2024, **16**, 9078–9087.
- C. Shuai, G. Liu, Y. Yang, F. Qi, S. Peng, W. Yang, C. He, G. Wang and G. Qian, A strawberry-like Ag-decorated barium titanate enhances piezoelectric and antibacterial activities of polymer scaffold, *Nano Energy*, 2020, **74**, 104825.
- C. C. Jin, D. M. Liu and L. X. Zhang, An emerging family of piezocatalysts: 2D piezoelectric materials, *Small*, 2023, **19**, 2303586.

29 T. Yao, J. Chen, Z. Wang, J. Zhai, Y. Li, J. Xing, S. Hu, G. Tan, S. Qi and Y. Chang, The antibacterial effect of potassium-sodium niobate ceramics based on controlling piezoelectric properties, *Colloids Surf., B*, 2019, **175**, 463–468.

30 F. Meng, X. Luo, Y. Shi, C. Wang, H. Zhu and J. Zheng, Piezoelectric performance of monolayer molybdenum disulfide carbon nanogenerator, *Colloids Surf., A*, 2024, **693**, 135961.

31 M. Shehzad, S. Wang and Y. Wang, Flexible and transparent piezoelectric loudspeaker, *npj Flexible Electron.*, 2021, **5**, 117451.

32 X. Chen, H. Xu, C. Liu, Z. Wang, R. Wang, J. Wang, R. Pan, J. Qi, Y. Wang and F. Meng, Synthesis and characterization of Vs-B/MoS<sub>2</sub> with double defects for efficient piezocatalytic antibiotic degradation and bacterial disinfection, *Chem. Eng. J.*, 2024, **498**, 155591.

33 Y.-X. Zhou, Y.-T. Lin, S.-M. Huang, G.-T. Chen, S.-W. Chen, H.-S. Wu, I. C. Ni, W.-P. Pan, M.-L. Tsai, C.-I. Wu and P.-K. Yang, Tungsten disulfide nanosheets for piezoelectric nanogenerator and human-machine interface applications, *Nano Energy*, 2022, **97**, 107172.

34 G. Singh, M. Sharma and R. Vaish, Flexible Ag@LiNbO<sub>3</sub>/PVDF Composite Film for Piezocatalytic Dye/Pharmaceutical Degradation and Bacterial Disinfection, *ACS Appl. Mater. Interfaces*, 2021, **13**, 22914–22925.

35 X. Ning, A. Hao, Y. Cao, J. Hu, J. Xie and D. Jia, Effective promoting piezocatalytic property of zinc oxide for degradation of organic pollutants and insight into piezocatalytic mechanism, *J. Colloid Interface Sci.*, 2020, **577**, 290–299.

36 Y. Wei, Y. Zhang, W. Geng, H. Su and M. Long, Efficient bifunctional piezocatalysis of Au/BiVO<sub>4</sub> for simultaneous removal of 4-chlorophenol and Cr(VI) in water, *Appl. Catal., B*, 2019, **259**, 118084.

37 Q. Nie, Y. Xie, J. Ma, J. Wang and G. Zhang, High piezocatalytic activity of ZnO/Al<sub>2</sub>O<sub>3</sub> nanosheets utilizing ultrasonic energy for wastewater treatment, *J. Cleaner Prod.*, 2020, **242**, 118532.

38 H. Liu, Y. Ye, Y. Zhang, X. Wang, X. Zhang and H. Liu, Y., Enhanced Piezoelectric Response in Monolayer Tungsten Disulfide, *Nano Lett.*, 2018, **18**, 1864.

39 C. Jin, D. Liu, J. Hu, Y. Wang, Q. Zhang, L. Lv and F. Zhuge, The role of microstructure in piezocatalytic degradation of organic dye pollutants in wastewater, *Nano Energy*, 2019, **59**, 372–379.

40 Q. Truong Hoang, V. Ravichandran, T. G. Nguyen Cao, J. H. Kang, Y. T. Ko, T. I. Lee and M. S. Shim, Piezoelectric Au-decorated ZnO nanorods: Ultrasound-triggered generation of ROS for piezocatalytic cancer therapy, *Chem. Eng. J.*, 2022, **435**, 135039.

41 B. Zhang, Z. Yang, S. Yang, Y. Xu, X. Tang, H. Mao, R. Dai and X. Liang, Construction of ZnO/Cu<sub>2</sub>O composites for enhanced antibacterial activity and analysis of antibacterial mechanism, *Inorg. Chem. Commun.*, 2024, **162**, 112182.

42 C. Montoya, A. Jain, J. J. Londoño, S. Correa, P. I. Lelkes, M. A. Melo and S. Orrego, Multifunctional dental composite with piezoelectric nanofillers for combined antibacterial and mineralization effects, *ACS Appl. Mater. Interfaces*, 2021, **13**, 43868–43879.

43 W. Ma, M. Lv, F. Cao, Z. Fang, Y. Feng, G. Zhang, Y. Yang and H. Liu, Synthesis and characterization of ZnO-GO composites with their piezoelectric catalytic and antibacterial properties, *J. Environ. Chem. Eng.*, 2022, **10**, 107840.

44 Y. Zhao, Y. Liu, R. Liao, P. Ran, Y. Liu, Z. Li, J. Shao and L. Zhao, Biofilm Microenvironment-Sensitive Piezoelectric Nanomotors for Enhanced Penetration and ROS/NO Synergistic Bacterial Elimination, *ACS Appl. Mater. Interfaces*, 2024, **16**, 3147–3161.

45 D. He, W. Wang, N. Feng, Z. Zhang, D. Zhou, J. Zhang, H. Luo, Y. Li, X. Chen and J. Wu, Defect-modified nano-BaTiO<sub>3</sub> as a sonosensitizer for rapid and high-efficiency sonodynamic sterilization, *ACS Appl. Mater. Interfaces*, 2023, **15**, 15140–15151.

46 J. Lei, C. Wang, X. Feng, L. Ma, X. Liu, Y. Luo, L. Tan, S. Wu and C. Yang, Sulfur-regulated defect engineering for enhanced ultrasonic piezocatalytic therapy of bacteria-infected bone defects, *Chem. Eng. J.*, 2022, **435**, 134624.

47 Z. Zhou, B. Li, X. Liu, Z. Li, S. Zhu, Y. Liang, Z. Cui and S. Wu, Recent Progress in Photocatalytic Antibacterial, *ACS Appl. Bio Mater.*, 2021, **4**, 3909–3936.

48 K. Wang, M. Lv, T. Si, X. Tang, H. Wang, Y. Chen and T. Zhou, Mechanism analysis of surface structure-regulated Cu<sub>2</sub>O in photocatalytic antibacterial process, *J. Hazard. Mater.*, 2024, **461**, 132479.

49 D. Liu, L. Li, B.-L. Shi, B. Shi, M.-D. Li, Y. Qiu, D. Zhao, Q.-D. Shen and Z.-Z. Zhu, Ultrasound-triggered piezocatalytic composite hydrogels for promoting bacterial-infected wound healing, *Bioact. Mater.*, 2023, **24**, 96–111.

50 T. Ding, F. Liu, H. Xin, Y. Chen, L. Kong, J. Han, D. Ma, Y. Han and L. Zhang, Pyro-piezoelectric effect of BaTiO<sub>3</sub> bio-nanocarrier for osteomyelitis therapy, *Nano Today*, 2024, **54**, 102069.

51 A. Banerjee, A. Mukherjee, N. Bag, P. Halder, I. Mondal, J. Roy, D. Mondal, S. Bardhan, A. Majumdar and S. Das, Ultrasonic vibration-assisted enhanced antibacterial activity of ZnO/Chitosan bio-nanocomposite, *J. Mol. Struct.*, 2024, **1298**, 136996.

52 K. Karthik, S. Dhanuskodi, C. Gobinath, S. Prabukumar and S. Sivaramakrishnan, Dielectric and antibacterial studies of microwave assisted calcium hydroxide nanoparticles, *J. Mater. Sci.: Mater. Electron.*, 2017, **28**, 16509–16518.

53 Z. Zhu, X. Gou, L. Liu, T. Xia, J. Wang, Y. Zhang, C. Huang, W. Zhi, R. Wang, X. Li and S. Luo, Dynamically evolving piezoelectric nanocomposites for antibacterial and repair-promoting applications in infected wound healing, *Acta Biomater.*, 2023, **157**, 566–577.

54 H. Luo, Z. Liu, C. Ma, A. Zhang, Q. Zhang and F. Wang, 2D/2D KNbO<sub>3</sub>/MoS<sub>2</sub> heterojunctions for piezocatalysis: Insights into interfacial electric-fields and reactive oxygen species, *J. Environ. Chem. Eng.*, 2023, **11**, 111521.

55 M. Wu, Z. Zhang, Z. Liu, J. Zhang, Y. Zhang, Y. Ding, T. Huang, D. Xiang, Z. Wang, Y. Dai, X. Wan, S. Wang, H. Qian, Q. Sun and L. Li, Piezoelectric nanocomposites for

sonodynamic bacterial elimination and wound healing, *Nano Today*, 2021, **37**, 101104.

56 H. Zhao, T. Zhong, W. Huang, X. Guo, P. Ma, T. Wu, J. He, L. Hu, D. Xia and C. He, Designing multi-functional MoS<sub>2</sub>/rGO piezocatalysts based on bacteria-catalyst topological interactions and electron pump effects for efficient water disinfection, *J. Cleaner Prod.*, 2024, **461**, 142597.

57 T. Song, X. Cai and Y. Zhu, Hydrogen production catalysed by atomically precise metal clusters, *Nanoscale*, 2024, **16**, 13834–13846.

58 X. Wang, N. Wang, J. Liao, X. Wang, A. Zou, Q. Chen, C. B. W. Li, J. Zhang, D. Wang and Y. Peng, Lead-Free (K, Na) NbO<sub>3</sub> Piezocatalyst with Superior Piezocatalysis and Large-Scale Production, *Adv. Funct. Mater.*, 2024, **34**, 2313662.

59 Z. Zhou, L. Sun, Y. Tu, Y. Yang, A. Hou, J. Li, J. Luo, L. Cheng, J. Li and K. Liang, Exploring Naturally Tailored Bacterial Outer Membrane Vesicles for Selective Bacteriostatic Implant Coatings, *Adv. Sci.*, 2024, 2405764.

60 J. Feng, X. Liu, K. Li, W. Zhao, W. Wang, S. Ge, H. Liu and J. Li, Intracellular delivery of piezotronic-dominated nanocatalysis to mimic mitochondrial ROS generation for powering macrophage immunotherapy, *Nano Energy*, 2024, **122**, 109287.

61 D. Mondal, S. Bardhan, N. Das, J. Roy, S. Ghosh, A. Maity, S. Roy, R. Basu and S. Das, Natural clay-based reusable piezo-responsive membrane for water droplet mediated energy harvesting, degradation of organic dye and pathogenic bacteria, *Nano Energy*, 2022, **104**, 107893.

62 J.-H. Chang, S.-Y. Shen, C.-D. Dong, B. Dakshinamoorthy and M. Kumar, Study on the efficacy of sterilization in tap water by electrocatalytic technique, *J. Appl. Electrochem.*, 2021, **51**, 539–550.

63 J. Liao, X. Lv, J. Zheng, H. Wang, Q. Chen, D. Gao, J. Bi and J. Wu, Constructing the relationship between microstructure and piezocatalysis in (K, Na)NbO<sub>3</sub> lead-free piezocatalyst, *Mater. Today Commun.*, 2023, **37**, 107564.

64 J. Wei, J. Xia, X. Liu, P. Ran, G. Zhang, C. Wang and X. Li, Hollow-structured BaTiO<sub>3</sub> nanoparticles with cerium-regulated defect engineering to promote piezocatalytic antibacterial treatment, *Appl. Catal., B*, 2023, **328**, 122520.

65 G. Khandelwal, A. Chandrasekhar, N. P. Maria Joseph Raj and S. J. Kim, Metal–Organic Framework: A Novel Material for Triboelectric Nanogenerator-Based Self-Powered Sensors and Systems, *Adv. Energy Mater.*, 2019, **9**, 201803581.

66 L. Ruan, Y. Jia, J. Guan, B. Xue, S. Huang, Z. Wu, G. Li and X. Cui, Highly piezocatalysis of metal-organic frameworks material ZIF-8 under vibration, *Sep. Purif. Technol.*, 2022, **283**, 120159.

67 J. Chen, L. Song, F. Qi, S. Qin, X. Yang, W. Xie, K. Gai, Y. Han, X. Zhang, Z. Zhu, H. Cai, X. Pei, Q. Wan, N. Chen, J. Wang, Q. Wang and Y. Li, Enhanced bone regeneration via ZIF-8 decorated hierarchical polyvinylidene fluoride piezoelectric foam nanogenerator: Coupling of bioelectricity, angiogenesis, and osteogenesis, *Nano Energy*, 2023, **106**, 108076.

68 S. Zhang, L. Wang, Y. Zhang, X. Yu, Y. Zhang, H. Li, J. Pei, Y. Zhao and Q. An, Breathable Bactericide Piezocatalyst Integrating Anode–Cathode Heterojunction Capacitance on a Piezoelectric–Conductive Film, *ACS Appl. Mater. Interfaces*, 2023, **15**, 3867–3881.

69 Q. Pan, Y. Zheng, Y. Zhou, X. Zhang, M. Yuan, J. Guo, C. Xu, Z. Cheng, A. A. A. Kheraif and M. Liu, Doping Engineering of Piezo-Sonocatalytic Nanocoating Confer Dental Implants with Enhanced Antibacterial Performances and Osteogenic Activity, *Adv. Funct. Mater.*, 2024, **34**, 2313553.

70 Y. Yu, Y. Zeng, Q. Ouyang, X. Liu, Y. Zheng, S. Wu and L. Tan, Ultrasound-induced abiotic and biotic interfacial electron transfer for efficient treatment of bacterial infection, *ACS Nano*, 2023, **17**, 21018–21029.

71 A. Jacobs, G. Renaudin, C. Forestier, J.-M. Nedelec and S. Descamps, Biological properties of copper-doped biomaterials for orthopedic applications: A review of antibacterial, angiogenic and osteogenic aspects, *Acta Biomater.*, 2020, **117**, 21–39.

72 D. Gao, J. Zhang, B. Lyu, L. Lyu, J. Ma and L. Yang, Poly(quaternary ammonium salt-epoxy) grafted onto Ce doped ZnO composite: An enhanced and durable antibacterial agent, *Carbohydr. Polym.*, 2018, **200**, 221–228.

73 Y. Han, H. Zhang, R. Yang, X. Yu, Z. Marfavi, Q. Lv, G. Zhang, K. Sun, C. Yuan and K. Tao, Ba<sup>2+</sup>-doping introduced piezoelectricity and efficient Ultrasound-Triggered bactericidal activity of brookite TiO<sub>2</sub> nanorods, *J. Colloid Interface Sci.*, 2024, **670**, 742–750.

74 Y. Fu, C. Li, Y. Cheng, Y. He, W. Zhang, Q. Wei and D. Li, Biomass aerogel composite containing BaTiO<sub>3</sub> nanoparticles and MXene for highly sensitive self-powered sensor and photothermal antibacterial applications, *Composites, Part A*, 2023, **173**, 107663.

75 J. Lin, L. Liu, Y. Peng, C. Wu, X. Yang and N. Zhou, Rigid-Flexible Coupling Modification Strategy Realized by Combining MXene with C-Coated Microsilicon for Long-Life Li-Ion Battery, *ACS Appl. Energy Mater.*, 2024, **7**, 1182–1191.

76 S. Ma, X. Li, J. Kong, X. Yu and X. Bai, Light-triggered bactericidal semiconductor nanomaterials: classification, modification and antibacterial strategies, *Appl. Mater. Today*, 2024, **39**, 102279.

77 X. Wang, H. Wang, J. Cheng, H. Li, X. Wu, D. Zhang, X. Shi, J. Zhang, N. Han and Y. Chen, Initiative ROS generation of Cu-doped ZIF-8 for excellent antibacterial performance, *Chem. Eng. J.*, 2023, **466**, 143201.

78 Q. Liu, L. Liu, D. Fan, S. Xie, C. Wang, X. Gou and X. Li, Self-powered biodegradable piezoelectric fibrous composites as antibacterial and wound healing dressings, *Appl. Mater. Today*, 2024, **37**, 102120.

79 B. Huo, J. Wang, Z. Wang, X. Zhang, J. Yang, Y. Wang, J. Qi, W. Ma and F. Meng, Bubble-driven piezo-activation of E-MoS<sub>2</sub>/PVDF piezoelectric microcapsule for antibiotic degradation with ultralow energy consumption, *J. Cleaner Prod.*, 2023, **419**, 138333.

80 S. Kumar, M. Sharma, A. Kumar, S. Powar and R. Vaish, Rapid bacterial disinfection using low frequency piezocatalysis effect, *J. Ind. Eng. Chem.*, 2019, **77**, 355–364.

81 Z. Wang, M. Xiang, B. Huo, J. Wang, L. Yang, W. Ma, J. Qi, Y. Wang, Z. Zhu and F. Meng, A novel ZnO/CQDs/PVDF

piezoelectric system for efficiently degradation of antibiotics by using water flow energy in pipeline: Performance and mechanism, *Nano Energy*, 2023, **107**, 108162.

82 S. Shi, Y. Jiang, Y. Yu, M. Liang, Q. Bai, L. Wang, D. Yang, N. Sui and Z. Zhu, Piezo-Augmented and Photocatalytic Nanozyme Integrated Microneedles for Antibacterial and Anti-Inflammatory Combination Therapy, *Adv. Funct. Mater.*, 2022, **33**, 202210850.

83 X. Xuan, S. Huang, M. Qin, J. Shen, L. Wang, X. Zhang, J. Zhang, X. Lu, Z. Hou, X. Gao, Z. Zhang and J. Liu, Defective ReS<sub>2</sub> Triggers High Intrinsic Piezoelectricity for Piezo-Photocatalytic Efficient Sterilization, *ACS Appl. Mater. Interfaces*, 2023, **15**, 55753–55764.

84 M. Chai, W. Tong, Z. Wang, Z. Chen, Y. An and Y. Zhang, Piezoelectric-Fenton degradation and mechanism study of Fe<sub>2</sub>O<sub>3</sub>/PVDF-HFP porous film drove by flowing water, *J. Hazard. Mater.*, 2022, **430**, 128446.

85 J. Xu, Q. Zhang, X. Gao, P. Wang, H. Che, C. Tang and Y. Ao, Highly Efficient Fe<sup>III</sup>-initiated Self-cycled Fenton System in Piezo-catalytic Process for Organic Pollutants Degradation, *Angew. Chem., Int. Ed.*, 2023, **62**, 202307018.

86 Y. L. Q. Zhang, Z. Zhao and J. Huang, Piezoelectric Fenton-like reaction for efficient bacterial inactivation: Enhanced catalytic performance of ZnO nanorods, *J. Hazard. Mater.*, 2022, **424**, 127472.

87 J. Jacob, N. More, C. Mounika, P. Gondaliya, K. Kalia and G. Kapusetti, Smart Piezoelectric Nanohybrid of Poly(3-hydroxybutyrate-*co*-3-hydroxyvalerate) and Barium Titanate for Stimulated Cartilage Regeneration, *ACS Appl. Bio Mater.*, 2019, **2**, 4922–4931.

88 R. Das, E. J. Curry, T. T. Le, G. Awale, Y. Liu, S. Li, J. Contreras, C. Bednarz, J. Millender, X. Xin, D. Rowe, S. Emadi, K. W. H. Lo and T. D. Nguyen, Biodegradable nanofiber bone-tissue scaffold as remotely-controlled and self-powering electrical stimulator, *Nano Energy*, 2020, **76**, 105028.

89 L. Ge, J. Xiao, W. Liu, G. Ren, C. Zhou, J. Liu, J.-J. Zou and Z. Yang, A Piezo-Fenton System with Rapid Iron Cycling and Hydrogen Peroxide Self-Supply Driven by Ultrasound, *Chem. – Eur. J.*, 2022, **28**, e202202494.

90 J. H. Liu, W. L. Qi, M. M. Xu, T. J. Thomas, S. Q. Liu and M. H. Yang, Piezocatalytic Techniques in Environmental Remediation, *Angew. Chem., Int. Ed.*, 2023, **62**, e202213927.